

1 **Pre-diagnosis plasma cell-free DNA methylome profiling up to seven years prior to clinical**
2 **detection reveals early signatures of breast cancer**

3
4 Nicholas Cheng^{1,2}, Kimberly Skead^{1,2}, Althaf Singhawansa^{4,5,6}, Tom W. Ouellette^{1,2}, Mitchell
5 Elliott^{4,5}, David W. Cescon^{4,5,6}, Scott V. Bratman^{6,7,8}, Daniel D. De Carvalho^{6,7}, David Soave^{1,3},
6 Philip Awadalla^{1,2,9,10}

- 7
8 1. Computational Biology, Ontario Institute for Cancer Research, Toronto, Ontario, Canada
9 2. Department of Molecular Genetics, University of Toronto, Toronto, Ontario, Canada
10 3. Department of Mathematics, Wilfrid Laurier University, Waterloo, Ontario, Canada
11 4. Department of Medicine, University of Toronto, Toronto, Ontario, Canada
12 5. Department of Medical Oncology, Princess Margaret Cancer Centre, University Health
13 Network, Toronto, Ontario, Canada
14 6. Princess Margaret Cancer Centre, University Health Network, Toronto, Ontario, Canada
15 7. Department of Medical Biophysics, University of Toronto, Ontario, Canada
16 8. Department of Radiation Oncology, University of Toronto, Toronto, Ontario, Canada
17 9. Ontario Health Study, Ontario Institute for Cancer Research, Toronto, Canada
18 10. Dalla Lana School of Public Health, University of Toronto, Ontario Canada

19
20 Corresponding author: Philip Awadalla (Philip.awadalla@oicr.on.ca)

21
22
23
24

25 Abstract

26 Profiling of cell-free DNA (cfDNA) has been well demonstrated to be a potential non-invasive
27 screening tool for early cancer detection. However, limited studies have investigated the
28 detectability of cfDNA methylation markers that are predictive of cancers in asymptomatic
29 individuals. We performed cfDNA methylation profiling using cell-free DNA methylation
30 immunoprecipitation sequencing (cfMeDIP-Seq) in blood collected from individuals up to seven
31 years before a breast cancer diagnosis in addition to matched cancer-free controls. We identified
32 differentially methylated cfDNA signatures that discriminated cancer-free controls from pre-
33 diagnosis breast cancer cases in a discovery cohort that is used to build a classification model.
34 We show that predictive models built from pre-diagnosis cfDNA hypermethylated regions can
35 accurately predict early breast cancers in an independent test set (AUC=0.930) and are
36 generalizable to late-stage breast cancers cases at the time of diagnosis (AUC=0.912).
37 Characterizing the top hypermethylated cfDNA regions revealed significant enrichment for
38 hypermethylation in external bulk breast cancer tissues compared to peripheral blood leukocytes
39 and breast normal tissues. Our findings demonstrate that cfDNA methylation markers predictive
40 of breast cancers can be detected in blood among asymptomatic individuals up to six years prior
41 to clinical detection.

42

43 Key words

44 Cell-free DNA, breast cancer, methylation, early cancer, liquid biopsy, pre-diagnosis, cfMeDIP-
45 Seq

46

47 Background

48 High morbidity and mortality rates associated with cancers is largely attributed to late-stage
49 diagnoses. Across most cancers, survival outcomes are significantly improved when tumours are

50 still localised to the tissue of origin at diagnosis [1]. However, effective population screening tools
51 for early cancer detection are currently limited to a few cancer types, notably breast, colorectal,
52 lung and cervical cancer [2,3]. For example, routine mammogram screening is currently
53 recommended to women biennially between the ages of 50-70 in Canada and remains the gold
54 standard for early breast cancer (BRCA) detection. Yet, breast cancer is still expected to be
55 responsible for 25.4% of female cancer cases, and 13.8% of all female cancer related deaths in
56 2022 [4]. Likewise, limited participation as well as high false positive rates, have raised concerns
57 of overdiagnosis and overtreatment of breast cancers following mammography [5-7].

58
59 Profiling cell-free DNA (cfDNA) derived from tumours in blood, also known as circulating tumour
60 DNA (ctDNA), is well demonstrated to be a potential non-invasive biomarker that can provide a
61 glimpse into the genetic and epigenetic landscape of a tumour's genome [8-12]. Sensitive liquid
62 biopsy assays examining tumour specific cfDNA methylation profiles are able to detect both early-
63 and late-stage cancers and inform on the tissue of origin of underlying tumours. In addition, some
64 studies have even combined cfDNA biomarkers with alternative markers such as multi-protein
65 panels or radiographic imaging to further improve diagnostic accuracy [11, 13]. Several studies
66 to date have shown the diagnostic potential of cfDNA methylation profiles for early breast cancer
67 detection by building targeted panels from bulk cancer tissue to profile and classify individuals
68 with established early-stage cancers [13-16]. However, as most cancers are often only detected
69 once patients are screened or become symptomatic, these studies have primarily been performed
70 using biologic samples collected from patients following clinical detection and diagnosis of a
71 malignant primary tumour. Profiling cfDNA in the pre-diagnostic context could allow us to better
72 understand the detectability of cancer biomarkers across cancer subtypes at the earliest stages,
73 however this requires application of new technologies to biologics collected from healthy
74 individuals prior to a cancer diagnosis.

75

76 Here, we profiled cfDNA methylation patterns in plasma samples collected from cohort
77 participants prior to a breast cancer diagnosis and matched cancer-free controls to identify and
78 assess cfDNA markers predictive of early breast cancers and breast cancer risk. We leverage the
79 Ontario Health Study (OHS), an Ontario-based longitudinal prospective cohort that collected
80 health and lifestyle information through self-reported questionnaires, and biologics including blood
81 plasma, from over 41,000 participants between 2009 and 2017 [17]. A particular advantage of the
82 OHS is that almost all participants provided consent to administrative health linkages at initial
83 recruitment into the study. We were able link health insurance numbers of recruited individuals to
84 administrative health registries to identify participants that developed breast cancer up to 7 years
85 after study recruitment and biologic donation. Using 1.6 mL of blood plasma from incident breast
86 cancer cases, in addition to matched controls, we analyzed and compared cfDNA methylomes in
87 pre-diagnosis blood plasma samples versus cancer-free samples. In this study, all sequencing
88 runs and analytics in the discovery cohort were performed with cases and controls concurrently
89 to minimize inflation of accuracy, sensitivity, and specificity. By retrospectively interrogating blood
90 samples collected prior to diagnosis, we assessed the earliest detectability and predictive
91 performance of cfDNA methylation markers for classifying participants harboring undetected
92 breast cancers and in stage IV breast cancers from an independent cohort.

93

94 Methods

95 **Cohort participants and demographics**

96 Peripheral blood was drawn from OHS participants upon recruitment to the study, and 1.6 mL
97 plasma was separated and collected within 48 hours into EDTA tubes, and immediately
98 cryopreserved at the OHS Biobank. Participants in OHS that had developed breast cancer
99 following recruitment to the study were identified by linking individuals to the Ontario Cancer
100 Registry through Cancer Care Ontario (CCO) using health insurance number, age, sex and name.
101 At the time of linkages, cancer registry data had been made available through the Ontario Cancer

102 Registry up until December 2017. All samples and participant data were deidentified and assigned
103 unique research IDs to prevent identification of study subjects prior to analysis. Original OHS and
104 CCO IDs are not known to anyone outside the research group. Breast cancers were confirmed
105 by histological analyses of tissue biopsies at the time of diagnosis, and immuno-histochemical
106 tests for hormone receptor status were reported in the pathology records of breast cancer cases.
107 In total, 110 incident breast cancer cases among participants diagnosed with breast cancer after
108 providing a blood sample at the time of enrollment were identified, in addition to 108 control
109 participants with no history of cancer at the time of study enrollment and throughout the study
110 follow up time (Fig. 1, Fig. S1, Supplementary Table 1 & Supplementary Table 2). Cancer-free
111 controls were matched to cases by age, sex, date of biologic collection, ethnicity, smoking status,
112 and alcohol consumption frequency were also selected. Additional plasma samples from 35
113 patients with established breast cancer were obtained from participants in the Ontario-wide
114 Cancer TArgeted Nucleic Acid Evaluation (OCTANE) study [18].

115

116 **Cell-free DNA methylation profiling**

117 Using 1.6 mL of plasma from pre-diagnosis breast cancer and selected cancer-free control
118 participants, cfDNA methylation patterns were profiled using a cell-free methylated DNA
119 immunoprecipitation sequencing protocol (cfMeDIP-Seq) to sequence methylated cfDNA
120 fragments [19-20]. The cfDNA from OHS and OCTANE samples was extracted from plasma using
121 the QIAamp Circulating Nucleic Acid Kit (Qiagen). 5-10ng of cfDNA was used as input to generate
122 methylated cfDNA libraries (IP libraries) along with an input control library (IC libraries). Quality of
123 incoming cfDNA was assessed using the Fragment Analyzer (Agilent) following the manufacturers
124 guidelines. 0.1ng of *Arabidopsis thaliana* DNA was added to samples prior to library preparation.
125 Combined samples were prepared using the KAPA Hyper Prep library protocol (Roche), with
126 standard End Repair & A-tailing and ligation of xGen Duplex Seq Adapter (IDT), followed by
127 incubation at 4°C overnight. Unmethylated lambda (λ) DNA was added to partially completed IP

128 libraries and enriched for methylated DNA using the MagMeDip Kit (Diagenode) and purified with
129 the IPure Kit v2 (Diagenode). Sample indices were added to IP and IC libraries via PCR.
130 Completed libraries were quantified by Qubit (Life Technologies) and Fragment Analyzer
131 (Agilent). Both IP and IC libraries underwent shallow sequencing (~20,000 reads) on the MiSeq
132 platform as a quality control step. IP libraries were sequenced to approximately 60M read pairs in
133 2x50bp mode on Novaseq platform (Illumina). To mitigate confoundment of biological signals from
134 technical artifacts associated with batch effects, cancer cases were batched together with control
135 samples during and across library preparation and sequencing runs.

136

137 **Raw sequencing read processing**

138 Following sequencing, the FASTQ raw reads were adapter trimmed, with unique molecular
139 identifiers (UMIs) appended to fastq headers using UMI Tools (version 0.3.3) [21]. The reads were
140 then aligned to hg38 using Bowtie2 (version 2.3.5.1) [22] in paired end mode at default settings.
141 Aligned SAM files were converted to BAM file format, indexed, and sorted using SAM tools
142 (version 1.9) [23]. Aligned reads were subsequently deduplicated according to alignment positions
143 and UMIs using UMI Tools.

144

145 **Quality control and sample inclusion**

146 One control sample was excluded from our study owing to mortality from non-cancer related
147 causes during study follow up. Five controls were excluded due to diagnoses of cancer pre-
148 disposing conditions that were identified from self-reported questionnaires during follow up. Three
149 control samples were excluded owing to diagnosis of another cancer following sample collection
150 and processing. Following library preparation, four samples were removed as no reads were
151 generated during the MiSeq quality control step. We retained and analysed all samples with more
152 than 10 million deduplicated reads. 39 samples were removed owing to Novaseq sequencing
153 instrument failure that resulted in poor sequencing yields. To assess enrichment efficiency, the

154 number of methylated and unmethylated Arabidopsis spike-ins aligned to F19K16 and F24B22
155 respectively were counted, and the proportion of methylated spike-ins generated out of the total
156 spike-ins were calculated. Seven samples with less than 95% of spike-in reads that were
157 methylated were excluded. An additional seven were samples owing to poor CpG enrichment
158 assessed through GoGe (< 1.75) and relH enrichment scores (< 2.7) calculated using MEDIPS
159 were also removed (See Supplementary Table 2 for quality control metrics and sample
160 information among remaining samples). Following quality control filtering, 82 pre-diagnosis breast
161 cancer cases and 70 cancer-free controls were retained for subsequent analyses. Additional
162 previously published cfMeDIP-Seq profiles from six head and neck cancers cases and five non-
163 cancer controls were used as non-breast cancer controls for validation [24].

164

165 **Computing cfMeDIP-Seq methylation signals**

166 To infer cfDNA methylation levels among pre-diagnosis breast cancers and control samples,
167 coverage profiles were generated for each sample across 300 bp non-overlapping binned tiled
168 windows from BAM files using MEDIPS (R package version 1.12.0) [25]. Cell-free DNA
169 methylation coverage profiles were library size normalized across all OHS, OCTANE and external
170 non-breast cancer samples using the DESeq2 R package version 1.30.1 [26]. Regions with no
171 coverage within a particular sample are assigned a count of 0. To reduce background noise,
172 publicly accessible data was used to remove potentially uninformative regions. Regions frequently
173 methylated in haematopoietic cells were inferred using whole genome bisulfite sequencing data
174 of peripheral blood leukocytes ($n = 78$) from the International Human Epigenetics Consortium
175 (IHEC) [27]. We averaged the level of methylation across all CpG sites within the same 300 bp
176 non-overlapping tiled window for each sample to infer the level of methylation within a specified
177 region. Regions with a methylation level greater than 0.25 averaged across PBL samples for each
178 cell type were excluded. Remaining 300-bp bins with at least six or more CpG sites located at

179 CpG islands, shores and shelves, or in FANTOM5 annotated promoters and enhancers, or UCSC
180 RepeatMasker repetitive elements were tested for differential methylation (Fig. S2) [28].

181

182 **Statistical analysis**

183 All statistical analyses were implemented in R, version 4.0.4.

184

185 **Pre-diagnosis breast cancer differential methylation calling, classifier building and** 186 **performance assessment**

187 OHS samples were divided into a discovery set (n = 67 cases and n = 59 controls) and validation
188 set (n = 15 cases and n = 11 controls). Discovery set samples were used to identify differentially
189 methylated regions (DMRs) and to build predictive models for classifying early breast cancers.
190 While remaining validation set samples from a held-out batch, processed independently from the
191 discovery cohort samples, were used as a test set to validate the discovery cohort signatures and
192 predictive model.

193

194 To evaluate the best approach for differential methylation calling and the optimal number of
195 features to train machine learning models for predicting breast cancer risk among pre-diagnosis
196 samples in discovery set samples, a repeated 10-fold cross validation (CV) was performed 100
197 times (Fig. S3) [29]. First, pre-cancer cases and control samples were divided into 10
198 approximately equal sized sets using stratified sampling, balancing the proportion of pre-
199 diagnosis cases by years prior to diagnosis following blood collection in each fold set. Iteratively,
200 for each fold in the CV procedure, one set was selected as the test set and the remaining nine
201 sets were designated as the train set (comprising 10% and 90% of participants respectively).
202 Within the train set folds, differential methylation calling was performed using a Wald test of the
203 coefficient from a negative binomial regression of cfMeDIP-Seq methylation level on train set case

204 and control status using DESeq2, adjusting for batch using surrogate variables and age as
205 covariates. Differential methylation variance was tested by performing Bartlett's test using
206 matrixTests (R package version 0.1.9.1) [30] between pre-diagnosis cases and controls. Features
207 were ranked according to p-values from respective tests selecting for regions with a minimum log
208 fold-change in methylation > 0.5 between cases and controls.

209
210 Iteratively, within each subsampling iteration, the top ranking 50 to 400 hypermethylated regions
211 identified from train set folds were used to construct a random forest model with Caret (R package
212 6.0) [31, 32] from library-size normalized discovery set sample methylation counts. The random
213 forest models were tuned using a nested 10-fold cross validation with 10-repeats iterating across
214 values from 5 to 50 for the number of features sampled to grow individual decision trees, and 250
215 to 1000 trees in the model to maximize the overall nested CV classification accuracy. The model
216 performance was then assessed by applying the predictive model to the held-out test fold to obtain
217 classification scores that reflected the proportion of decision trees predicting the sample as breast
218 cancer. The 10-fold CV procedure was repeated 100 times with different fold-splits to get stable
219 average estimates of cross-validated predictive performance. Differential methylation calling,
220 classifier building and assessment of predictive performance was effectively repeated 1000 times
221 with different sets of cases and controls in the train folds across each iteration. The test-fold
222 classification scores across each of the 100 CV repeats were averaged for each sample. A
223 bootstrapped area under the receiver operating characteristic curve (AUC) was calculated by
224 subsampling 67 cases and 59 controls with replacement, repeated for 3000 bootstraps. The final
225 bootstrap AUC was calculated by taking the median AUC, while 95% confidence intervals were
226 calculated by taking 2.5% and 97.5% percentiles.

227
228 To incorporate the follow-up time of controls, the time to diagnosis among the pre-diagnosis
229 cancer cases, as well as the proportion of true negative cases in the population, the concordance

230 index (C-index: the probability that for any pair of individuals, the individual with the higher
231 estimated risk score will have the earlier diagnosis time) [33] and time-dependent AUCs (AUC(t))
232 were computed [34]. Owing to the outcome and age dependent sampling used in the study, the
233 artificial case-to-non-case ratio in our sample was not representative of the Canadian adult
234 population. Sampling weights were calculated to adjust for this sampling bias in the time-
235 dependent model assessment analysis using age specific cumulative breast cancer incidence
236 rates from the Canadian Cancer Registry, in addition to all-cause mortality rates in Ontario
237 reported by Statistics Canada. Kaplan-Meier estimates weighted according to age-specific breast
238 cancer incidence for the corresponding follow-up times in the Canadian population were also
239 computed to assess whether averaged test-fold classification scores were predictive of time to
240 cancer diagnosis. Samples were stratified into a high risk and low risk group according to whether
241 they were assigned a classification score above or below 0.638 respectively. The cut off was
242 determined by optimizing sensitivity while limiting false positive rates at 5%. Cumulative
243 probabilities of developing breast cancer across timepoints were estimated by fitting a Cox
244 Proportional Hazard (CoxPH) model using the *cph* function (rms R package version 6.3) on the
245 discovery set with classification scores as predictors.

246

247 **Validation of discovery cohort signatures**

248 To validate the predictive performance of pre-diagnosis cfDNA hypermethylated regions, the
249 mean p-value and log fold-change (logFC) was calculated across the 1000 repeated differential
250 methylation calls within the discovery cohort CV procedure. The top ranking features were used
251 to build a random forest model from all discovery cohort samples and tuned using a nested CV in
252 the same way described above to optimize the tree number and number of subsampled regions
253 for each tree. To infer whether pre-diagnosis cfDNA DMRs were agreeable with established
254 cancers, predictive models were further assessed on late-stage breast cancer cases (n = 35) from
255 OCTANE [18] and external head and neck cancer cases [24] (n = 6), and cancer free controls (n

256 = 5). Predicted risk scores in the validation sets were used to calculate AUROCs to assess
257 classification performance and weighted Kaplan-Meier estimates to assess the performance for
258 predicting the absolute risk for developing breast cancer. The observed cumulative incidence
259 rates were compared to those estimated by the discovery set CoxPH model applied to the
260 validation samples.

261

262 **Overlap between pre-diagnosis cfDNA hypermethylated regions and bulk breast cancer** 263 **tissue methylome**

264 To assess whether the selected predictor regions used to build the classification model were
265 potentially derived from breast cancer tissue, the number of overlapping hypermethylated regions
266 was calculated between pre-diagnosis breast cancer cfDNA and bulk breast cancer tissue relative
267 to adjacent breast normal (ABRNM), healthy breast normal (HBRNM) tissue, and peripheral blood
268 leukocytes (PBL) using publicly accessible 450k DNA methylation array data. Solid breast cancer
269 and normal tissue raw IDAT files were downloaded from the TCGA data portal, and PBL from the
270 GeoExpression Omnibus (GSE87571 and GSE42861), in addition to healthy and adjacent normal
271 tissues (GSE88883, GSE101961 & GSE66313). IDAT files were processed to generate beta
272 methylation values from IDAT files using Minfi (1.36.0 R package) [35] and normalised using the
273 *preprocessFunnorm* function. To test for differentially methylated CpG sites between paired
274 healthy and tumour biopsies, an F-test was performed using the *DMPFinder* function from Minfi
275 across 485,512 CpG sites. Significantly differentially methylated regions were defined as CpG
276 sites with an absolute difference in methylation of greater than 0.1 and Bonferroni adjusted p-
277 value of less than 0.0001. Differential methylation calling between all breast cancer and breast
278 normal tissue, as well as between breast cancer tissue and PBL was also performed using the
279 *DMPFinder* function from Minfi between all samples from each respective group to identify
280 additional breast cancer specific markers. A permutation analysis was performed to infer whether
281 overlaps were significant, by comparing the observed overlap with the overlap between

282 significantly hypermethylated bulk tissue DMRs and randomly selected background cfDNA
283 regions (repeated 3000) times to obtain a background distribution for z-score normalization and
284 to calculate corresponding p-values. Additional BRCA, ABRNM, and HBRNM tissue data profiled
285 from the same study (GSE69914) with processed Beta methylation values was also analyzed as
286 described above. Predictor regions were annotated for genomic contexts using Annotatr (R
287 package version 1.24.0).

288

289 Results

290 **Discovery cohort pre-diagnosis breast cancer classification predictive performance;** 291 **internal cross-validation**

292 Most early cancer detection studies to date typically use a pre-designed enrichment panel to
293 target cancer tissue specific differentially methylated genomic loci prior to methylation profiling
294 [13-15]. In this study, we instead utilized cfMeDIP-Seq to interrogate genome-wide methylation
295 profiles, enabling the detection of both cfDNA specific methylation markers derived from tumours
296 and differentially methylated regions from non-tumour material potentially predictive of breast
297 cancer risk. To reduce background noise, we applied biological filters to remove potentially
298 uninformative genomic regions prior to differential methylation calling (Fig. S2). Loss of epigenetic
299 stability and increased stochasticity across the genome have been observed in pre-malignant and
300 early cancer tissue [36, 37]. Likewise, we suspect that in pre-diagnosis cfDNA samples not all
301 regions hypermethylated in cancer tissues will be observed, nor will we observe consistent
302 genomic regions to be impacted by methylation changes across pre-symptomatic individuals.
303 Therefore, we compared two approaches for differential methylation calling to rank and select
304 regions in the discovery cohort for training predictive models; the Wald test of the negative
305 binomial coefficient to test for changes in mean methylation level between groups, and the
306 Bartlett's test identifying differential variance in methylation to improve detection of sparse
307 predictor regions.

308

309 To iteratively identify and assess, using multivariate predictive models, whether cfDNA
310 hypermethylated regions can accurately predict an individual's risk of developing breast cancer,
311 we performed 100 repeated 10-fold CV procedures in the discovery cohort (Fig. S3). As the
312 predictive performances can be highly variable depending on which observations are included in
313 the train set and test set, a repeated CV approach can obtain stable average estimates as well
314 as the uncertainty of the cross-validated predictive performance in held-out test folds among
315 discovery cohort samples. In practice, a diagnostic screening tools aims to minimize false positive
316 rates while maximizing sensitivity to prevent overdiagnoses, thus we assessed the optimal
317 number of predictors and best feature selection approach that achieved the highest sensitivity at
318 95% specificity. Across all CV repeats, random forest classifiers trained with the top 150
319 hypermethylated regions from the Wald's test achieved the highest average sensitivity at 26.9%
320 (95% CI 0.9%-49.3%) while retaining 95% specificity for predicting breast cancer development on
321 test-fold samples (Fig. 2, Fig. S4). The averaged classification performance from bootstrapped
322 classification scores in discovery cohort samples achieved a mean binary classification AUC
323 across all breast cancer types, ages and varying pre-diagnosis time intervals of 0.724 (95% CI
324 0.636-0.810) (Fig. 2A). Further, the diagnostic classifiers trained with top 150 ranking
325 hypermethylated regions achieved an average C-index of 0.704 (95% CI 0.647-0.758) across the
326 repeated 10-fold CV iterations up to seven years prior to diagnosis in test set folds (Fig. 2B). The
327 diagnostic classifiers performed consistently well among cases diagnosed at stage I, achieving a
328 mean AUC of 0.725 (95% CI 0.626-0.824) and mean C-index of 0.704 (95% CI 0.655-0.757) (Fig.
329 2C). Notable differences in predictive performance across different breast cancer subtypes were
330 also observed when stratifying predictive performance by hormone receptor (HR) positive (n = 43
331 cases; 64.2%) and HR negative (n = 7 cases; 10.4%) breast cancers. Discovery cohort classifiers
332 performed better identifying early HR positive breast cancer cases using pre-diagnostic blood
333 cfDNA methylation signatures, detecting on average 32.6% of cases (95% CI 8.7%-50%) at 95%

334 specificity compared to an average sensitivity of 14.3% (95% CI 0%-43.2%) for HR negative
335 cancers (Fig. 2C).

336
337 Typically, all women between the ages of 50-70 are recommended to receive mammograms
338 biennially in Canada, however mammographic screening guidelines for women aged 40-49
339 remains controversial as The Canadian Task Force on Preventive Health Care recommended
340 against routine screening of women under 50 in their 2018 guidelines [7]. To address the
341 differences in routine care within the cohort, we specifically evaluated whether individuals
342 diagnosed at ages 35 to 50 in the discovery set, preceding the age of mammographic screening
343 eligibility in Ontario, could also benefit from cfDNA methylation tests for early breast cancer
344 detection. When stratifying binary classification performance according to age of diagnosis,
345 individuals diagnosed between the ages 35 to 50 (n = 16 cases) were classified with an AUC of
346 0.775 (95% CI 0.624-0.895), detecting 25% (95% CI 6.2%-62.5%) at 95% specificity, and a C-
347 index of 0.743 (95% CI 0.633-0.850) (Fig. 2C). Furthermore, within the discovery cohort, 35 cases
348 reported to have a negative breast mammography screen result within six months to one year
349 before providing a blood sample to the OHS (Fig. 1B). Stratifying the classification performance
350 for cases with negative mammogram results within one year of providing blood samples (Fig. 2C)
351 reveals classifiers achieve an AUC of 0.691 (95% CI 0.581-0.803), and a 20% sensitivity (95% CI
352 5.7%-41.0%) at 95% specificity, highlighting that cfDNA methylation markers can be predictive of
353 breast cancers prior to mammogram detection.

354
355 The average classification scores assigned by predictive models in each cross-validated fold of
356 the 100 repeats were also highly predictive of cancer-free survival. Due to the inflated ratio of
357 cases to controls in our study, unweighted KM curves will report inaccurate cancer-free survival
358 probabilities, particularly in low-risk groups as the proportion of cases to controls is significantly
359 lower in OHS and across the Canadian population (Fig. S5B-E). As such, we weighted case and

360 control samples by the age specific cumulative breast cancer incidence rates, adjusted for the all-
361 cause mortality rates in Ontario. Using a classification score cut off of 0.648 to stratify samples
362 using a weighted Kaplan-Meier (KM) estimate, which retains 95% specificity among discovery
363 cohort samples (Fig. S5A), we demonstrate significant association between high classification
364 scores and cancer-free survival rates (log-rank test $p = 9.15 \times 10^{-27}$) particularly in HR positive
365 breast cancers cases (log-rank test $p = 9.70 \times 10^{-27}$) and cases diagnosed between ages 35 to 50
366 (log-rank test $p = 3.4 \times 10^{-31}$) (Fig. 2D-E & Fig. S5G-H). Similarly, when estimating the cumulative
367 incidence rate of developing breast cancer within varying time points between high risk
368 (classification score ≥ 0.648) and low risk (classification score < 0.648) groups using a CoxPH
369 model, we found that individuals with a high risk score had on average an 11.1% (5.7%-16.1%)
370 chance of developing breast cancer within five years (Supplementary Table 3). Indeed, our
371 observed cumulative incidence was consistent with our estimated incidence at up to 4 years, after
372 which the observed incident was significantly higher owing to limited control samples with long
373 censorship times being predicted in the high risk group. Collectively, our findings reveal that
374 hypermethylated cfDNA signatures identified from pre-diagnosis samples can be predictive of
375 breast cancer development in our discovery cohort.

376

377 **External test set validation of discovery cohort differentially methylated regions and breast** 378 **cancer diagnostic classifier**

379 To validate whether pre-diagnosis cfDNA hypermethylated regions could predict the risk of an
380 individual developing breast cancer, we built a random forest classifier trained using all discovery
381 cohort samples and assessed on the held-out validation set of pre-diagnosis cases and controls
382 that were processed independently from samples in the discovery set. As the top 150
383 hypermethylated regions from the Wald's test achieved the highest average sensitivity in the
384 discovery set across internal CV repeats, we selected the same number of top ranking features
385 to build a classifier to predict breast cancer development in the OHS validation set samples.

386 Predictor regions used to train the model were selected by ranking hypermethylated regions
387 according to the mean p-value from the Wald's test across the 1000 repeated subsampling
388 differential methylation calls for each region within the discovery set. The diagnostic classifier
389 trained using the top 150 hypermethylated regions accurately discriminated validation set pre-
390 diagnosis breast cancer cases from controls, achieving an AUC of 0.930 (0.815-1.000) among
391 pre-diagnosis test set samples. Using the classification score cut off of 0.648, determined
392 previously from discovery set samples, we classified 53.3% of samples at a 0% false positive rate
393 (Fig. 3A-C). Test set sample classification scores assigned by the diagnostic classifiers were also
394 significantly higher ($p = 4.1 \times 10^{-5}$) in pre-diagnosis cases relative to controls (Fig. 3B). Interestingly,
395 all test set OHS samples with a classification score of over 0.648, selected previously from
396 discovery cohort samples, developed breast cancer within 6 years of blood sampling,
397 demonstrating cfDNA methylome signatures can be predictive of breast cancer risk (Fig. 3D).
398 Using the CoxPH model fitted from the discovery set, samples in the validation set high risk group
399 had an average estimated 9.2% (4.7%-13.4%) chance of being diagnosed with breast cancer
400 within 5 years. Owing to limited sample sizes, the average incident rate among high risk group
401 samples was underestimated compared to the observed incident rate, which were considerably
402 higher as no validation set control samples were assigned in the high risk group. Consequently,
403 further examination in a larger cohort is needed to assess the calibration of estimated risk
404 incidence.

405
406 We further evaluated the performance of the diagnostic classifier on an independent test set
407 comprised of stage IV breast cancer cases (n=35) profiled at the time of enrollment into OCTANE,
408 head and neck squamous cell carcinoma (HNSC) cases (n=6), and a set of non-cancer controls
409 (n=5) from samples profiled by *Burgener et al* [18, 24]. The classifier achieved an AUC of 0.912
410 when predicting on individuals with established late-stage breast cancer against non-breast
411 cancer samples regardless of subtyping (Fig. 3E). Interestingly, the classifiers performed better

412 in detecting HR positive breast cancers (AUC=0.963) compared to HR negative (AUC=0.868)
413 among the external test samples, consistent with the discovery cohort classification performance.
414 Using a classification score cut-off of 0.648, the classifiers detected HR positive breast cancers
415 at 76.4% sensitivity and HR negative breast cancers at 65.0% sensitivity, while retaining a
416 specificity of 100% for non-breast cancer samples including head and neck cancer cases (Fig.
417 3F-G), indicating that the pre-diagnostic breast cancer cfDNA methylation signatures are largely
418 agreeable with late stage malignancies.

419

420 **Differentially methylated regions in pre-diagnosis breast cancer cfDNA reflects breast** 421 **cancer epigenome**

422 We next assessed whether the top 150 ranked cfDNA hypermethylated predictor regions
423 identified from discovery cohort samples were concordant with breast cancer tissue
424 hypermethylated regions. However, as participant tumour biopsies at the time of diagnosis were
425 not available, we instead leveraged publicly available bulk breast cancer, adjacent breast normal,
426 healthy breast normal and PBL DNA 450k methylation array data. Presumably, if the cfDNA
427 hypermethylated markers were derived from breast cancer tissue, the same regions would be
428 concordantly hypermethylated when comparing bulk breast cancer tissue methylomes against
429 PBLs, as cfDNA from normal breast tissue is typically shed at extremely low frequency in healthy
430 individuals. Across the top 150 pre-diagnosis breast cancer cfDNA hypermethylated regions, 75
431 regions contained at least one CpG site profiled by the DNA 450k methylation array spanning 156
432 CpG Sites. The difference in methylation between TCGA bulk breast cancer tissues (n = 846) and
433 PBLs (n = 628) across the 156 CpG sites overlapping the 75 cfDNA hypermethylated regions
434 were computed against the cfDNA log-fold change in methylation (Fig. 4A), revealing that
435 hypermethylated regions in pre-diagnosis breast cancer cfDNA were concordantly
436 hypermethylated in bulk breast cancer tissue relative to PBLs. Similarly cfDNA hypermethylated

437 regions can also discriminate bulk breast cancer tissue from PBLs and bulk breast normal tissues
438 (Fig. S6).

439
440 To further investigate the overlap in hypermethylated regions between cfDNA and
441 hypermethylated regions in bulk breast tissue, we identified significant DMRs (FDR < 0.0001 &
442 absolute methylation difference > 0.1) in 450k methylation array breast cancer tissue relative to
443 PBLs. Among the 75 hypermethylated cfDNA regions, 47 (62.7%) regions overlapped with
444 significantly hypermethylated regions in 450k methylation array bulk breast cancer tissue relative
445 PBLs (Fig. 4B). To further evaluate whether the enrichment in hypermethylated regions between
446 cfDNA and bulk breast cancer tissue methylation array profiles were significant, a permutation
447 test was performed by comparing the observed number of overlapping regions to the expected
448 overlap if random background cfDNA regions were selected. Most notably, only regions that were
449 concordantly hypermethylated in pre-diagnosis cfDNA and in bulk breast cancer relative to PBLs
450 tissue were significantly ($p < 0.01$) overlapping (Fig. 4B), whereas hypomethylated regions were
451 not significantly enriched. Stratifying the enrichment by CpG island, shore, shelf, and open sea
452 regions further revealed that the overlapping hypermethylated regions were most enriched among
453 CpG islands, concordant with previous observations of hypermethylated regions in cancers being
454 primarily observed in CpG islands (Fig. 4C) [36, 38]. Likewise, computing the overlap between
455 the 75 hypermethylated cfDNA and significantly hypermethylated regions in bulk BRCA relative
456 to ABRNM (Fig. 4D, Fig. S7E) and HBRNM (Fig. S7A & Fig. S8A) revealed 29 and 36 significantly
457 overlapping regions respectively indicating that predictive cfDNA methylation markers consisted
458 of regions uniquely hypermethylated in breast cancer tissue (Fig. 4E). To further ensure that the
459 overlap wasn't by chance or due to confoundment, as the bulk breast cancer and breast normal
460 tissues methylation data were from separate studies, we recalculated the overlapping
461 hypermethylated regions using bulk BRCA, ABRNM and HBRNM collected and processed from
462 the same study (GSE69914). Consistent with the combined methylation array datasets, the cfDNA

463 hypermethylated regions were also significantly overlapping with regions hypermethylated in
464 BRCA relative to ABRNM (Fig. S7F & Fig. S8E) and HBRNM (Fig. S7G & Fig. S8F), particularly
465 among CpG island regions.

466

467 We observed that many of the hypermethylated cfDNA regions mapped to promoter regions of
468 tumour suppressor genes including GATA4, ZNF471 and SFRP, as well as in previously reported
469 cfDNA breast cancer methylation markers (Fig. S9, Supplementary Table 4). Among proximal
470 gene targets of hypermethylated cfDNA DMRs, various genes with dysregulated methylation were
471 also inversely correlated with changes in expression between TCGA breast cancer and normal
472 tissue among overlapping CpG sites, indicating that early changes in methylation detected from
473 cfDNA may directly alter expression of these genes (Fig. S10). For example, ICAM2 expression
474 has been implicated as a tumor suppressor that inhibits cancer cell invasion and migration,
475 however we found an increase in methylation that directly correlated with a decrease in
476 expression in breast cancer tissue [39]. Likewise, promoter methylation of genes such as *CDKL2*
477 has been highlighted as a cfDNA methylation marker for triple negative breast cancers [15].

478

479 We further compared whether the identified overlapping hypermethylated cfDNA markers were
480 specific to breast cancer tissue or potentially applicable to multiple cancers by calculating
481 overlapping hypermethylated regions in pre-diagnosis cfDNA and in TCGA cancers across 13
482 different tissues relative to PBL methylation profiles (Fig. 4F & Fig. S11). Pre-diagnosis
483 hypermethylated cfDNA markers in CpG island regions were most significantly enriched in breast
484 tissue for both cancer and normal tissue relative to other tissue types (Fig. 4F-G), indicating that
485 the hypermethylated CpG island regions detected in pre-diagnosis breast cancer cfDNA are likely
486 specific to breast cancer tissue. However, we also observed significantly overlapping
487 hypermethylated regions in other bulk cancer tissue types relative to PBL when including non-

488 CpG island regions, which may suggest potential pan-cancer applications among captured
489 markers.

490

491 Discussion

492 Using cfMeDIP-Seq to profile cfDNA methylomes, we were able to capture cfDNA methylation
493 signatures predictive of breast cancer development prior to clinical presentation and even in cases
494 with a negative mammogram screen within a year before blood collection. We highlighted the
495 predictive performance of using pre-diagnosis DMRs to classify individuals with underlying breast
496 cancers within a discovery cohort and for predicting the absolute risk of an individual developing
497 breast cancer within five years. We also demonstrate that these markers are detectable prior to
498 mammogram detection and performs particularly well in detecting early breast cancers among
499 women under the age of 50, for whom existing screening mammography programs are not
500 universally recommended. Furthermore, we were able to validate the performance of top ranking
501 hypermethylated regions by accurately discriminating a held-out batch of pre-diagnosis cases
502 from controls at 53.3% sensitivity while retaining 100% specificity. Despite this, we acknowledge
503 that the pre-diagnosis validation set sample sizes were small and additional validation of identified
504 biomarkers will need to be further investigated in independent studies with larger cohorts. Our
505 pre-diagnosis signatures are also highly generalizable to established metastatic breast cancers,
506 providing further evidence that these signatures are related to the underlying malignancy.
507 Likewise, the cfDNA methylation classifiers can also discriminate breast cancers from head and
508 neck cancers cases, although follow-up investigations will be necessary to assess the specificity
509 of our markers as they relate to cancer type and histology. We found that among the top 150
510 cfDNA hypermethylated regions detected in the discovery set, hypermethylated cfDNA regions at
511 CpG island were the most significantly enriched for in breast cancer tissue relative to PBLs and
512 normal breast tissues, revealing that the detected cfDNA hypermethylated regions captured in
513 pre-diagnosis samples are partially reflective of breast cancer methylomes. However, it should be

514 noted that among the top 150 hypermethylated regions identified from pre-diagnosis cases, only
515 62.7% of regions were concordantly hypermethylated in breast cancer tissue, which may implicate
516 other non-breast cancer tissue markers being predictive of breast cancer risk among remaining
517 non-overlapping regions. It is likely that other phenotypes such as paraneoplastic syndrome,
518 changes in the tumour microenvironment or other changes in immune profiles, may also
519 contribute, and improve risk prediction. Additional investigations deconvoluting immune profiles
520 and other tissue types from the detected cfDNA methylation markers will be needed to further
521 investigate the sources of non-overlapping regions.

522
523 There has been an increasing consensus among recent studies that cfDNA methylation profiles,
524 often combined with other biomarker or imaging-based approaches, can yield the best predictive
525 performance for detecting cancers at early stages [12]. However, to implement liquid biopsies for
526 population screening of cancers, the viability of existing assays and predictive models needs to
527 be demonstrated in biologic specimens collected prior to a cancer diagnosis. Our work builds on
528 major investments made to establish large longitudinal population cohorts that store samples
529 collected from healthy individuals at the time of study recruitment. By linking participants to
530 administrative data routinely collected in public health settings in Canada, we can follow up and
531 identify the occurrence of morbidities such as cancers. These types of cohort resources allow for
532 interrogation of pre-diagnosis biologic samples, as we described here using developments in
533 cfDNA methylation profiling assays and can be similarly extended to other cancers, as
534 demonstrated using OHS incident prostate cancer samples [40], and alternative emerging
535 methodologies interrogating blood biomarkers such as cell-free RNA, proteins, and metabolites.

536
537 Several recent studies have profiled plasma cfDNA methylation profiles of breast cancers for early
538 cancer detection, however these studies are primarily sampled from patients after clinical
539 detection or formal diagnoses, and typically use a pre-designed enrichment panel to target

540 specific genomic loci [13-16]. To date, only one study has profiled breast cancer plasma collected
541 prior to clinical detection: in that investigation using a single methylome marker, reported
542 sensitivities were between 5-12% with 88% specificity among samples collected two to three
543 years before diagnosis [41]. Comparatively, our predictive models achieve a mean sensitivity of
544 60% at 100% specificity for classifying test set breast cancer cases diagnosed up to six years
545 following blood plasma profiling. Acknowledging the sample size of pre-diagnosis test samples
546 was small, additional independent studies are needed to further validate the utility of cfDNA
547 methylation markers in pre-diagnosis samples. While we reported higher sensitivity for HR
548 positive breast cancer in both the discovery and late-stage breast cancer samples, existing
549 methylome profiling of plasma samples collected at the time of cancer diagnosis, and presumably
550 more advanced breast cancer patients have typically noted better classification performance
551 among HR negative breast cancers relative to HR positive [15, 42]. As the majority of breast
552 cancers are HR positive, the incidence rate of HR negative breast cancer in the OHS is relatively
553 low, and we suspect a poorer predictive performance among HR negative breast cancers may
554 arise from biasing toward selected features associated with the more numerous HR positive
555 breast cancers. Alternatively, considering that HR positive breast cancers typically have slower
556 doubling times, less aggressive cancers may be present for longer but remain undetected by
557 mammograms until reaching visible sizes allowing for a longer window of opportunity for detection
558 at an early stage and age. Conversely, aggressive cancers which develop and expand more
559 rapidly, may have a shorter window of opportunity for detection at an early stage.

560

561 The batching of case and control groups during sequencing are often not reported across early
562 cancer detection studies. Unfortunately, internal model performance can often be inflated if cases
563 and controls are processed in separate batches. When case and control groups are perfectly
564 confounded between batches, signals associated with technical artifacts can often drive
565 separation of case and control groups in both training and testing samples, consequently

566 conflating predictive performances [29, 43]. Accordingly, we profiled our cases with control
567 samples between sequencing runs in this study, in addition to using a repeated cross-validation
568 approach to estimate the uncertainty of predictive performances. Likewise using held-out a batch
569 of pre-diagnosis cases and control samples, we demonstrate that the captured markers are
570 predictive of breast cancer in an independent set of samples, and similarly demonstrate that the
571 developed classifiers were also highly robust for the identification of established breast cancers
572 from a separate cohort. False-positive predictions in our cohort may still represent
573 misclassifications of control samples with undetected underlying cancers, owing to variable follow-
574 up duration among cancer-free controls (Supplementary Table 2).

575
576 Additionally, the following limitations of the current study should be considered when interpreting
577 our findings. Firstly, 1.6 mL of plasma was used per participant for this study, which is a substantial
578 amount of biobanked material, but larger plasma volumes would likely increase the number of
579 ctDNA fragments captured and further improve detection sensitivity. Owing to the prospective
580 nature of the OHS cohort, our sample sizes of pre-diagnosis cancers were limited by the incidence
581 rate of the cancer among the study population with a cryopreserved blood sample, acknowledging
582 that these incident cases will accrue with time. Additionally, not all cancer-free control samples
583 were followed up for the same duration owing to our matching of controls to cases by sample
584 collection time. While we followed all controls up to 2019 to ensure that they were alive and free
585 of cancer, it is possible that controls with shorter follow up times may have underlying undetected
586 cancers that had yet to be diagnosed as suggested by the lack of high risk samples assigned in
587 the high risk group according to classification scores in either the discovery or validation sets.
588 Consequently, this may inflate the false positive rate by mislabelling control samples with
589 undiagnosed cancers. Likewise, the false negative rate may also be inflated by reducing the
590 power for detecting cancer specific DMRs if controls with undiagnosed cancers harbored the
591 same hypermethylated regions with pre-diagnosis cases.

592

593 Conclusions

594 Despite the current limitations described above, genome-wide cfDNA methylation profiling of pre-
595 diagnosis breast cancer plasma samples reveals detectable signatures that are predictive of
596 breast cancer risk up to six years prior to diagnosis. Currently, breast cancer is one of the few
597 cancer types with an established population screening tool owing to its associated reduction in
598 mortality. Consequently, most breast cancers are typically diagnosed at stage I or II as seen in
599 the OHS cohort and across the population. While mammograms are currently the gold standard
600 for early breast cancer screening achieving a 92% sensitivity and 92% specificity in Ontario [44],
601 low adherence to screening guidelines is recognized, substantial physical and personnel
602 resources are required to deliver such screening, and low-dose radiation exposure may also
603 increase the risk of future breast cancer development [45]. A liquid biopsy-based approach could
604 not only enable simultaneous detection of multiple cancer types, but also mitigate risks associated
605 with radiographic imaging approaches, and be relevant to groups of individuals where
606 mammographic screening methods are not currently recommended. While it is unclear whether
607 diagnoses prior to mammographic detection will further improve prognostic outcomes, detection
608 of breast cancer signatures up to six years prior to a stage I or II diagnosis presents potential
609 opportunities for early pre-symptomatic detection and intervention among other cancer types with
610 no reliable screening tool. While sample sizes of our validation sets are limited in our study, we
611 find that methylation signatures concordant with breast cancer tissue can be detected in cfDNA
612 preceding mammogram detection. Indeed, future applications of liquid biopsies for early cancer
613 detection will require identifying the tissue of origin of underlying cancers. Likewise, profiling of
614 pre-diagnosis plasma from individuals with other cancer types will allow for identifying tissue-
615 specific markers and the development of tissue of origin classifiers, similar to those demonstrated
616 in existing studies classifying samples with established cancers.

617

618 Abbreviations

619 **ABRNM:** Adjacent Breast Normal

620 **AUC:** Area Under the Receiver Operating Characteristic Curve

621 **AUC(t):** Time-dependent Area Under the Receiver Operating Characteristic Curve

622 **HBRNM:** Healthy Breast Normal

623 **BRCA:** Breast Cancer

624 **cfDNA:** Cell-free DNA

625 **C-index:** Concordance Index

626 **CoxPH:** Cox Proportional Hazard

627 **CV:** Cross-validation

628 **DMR:** Differentially Methylated Regions

629 **GEO:** Geo Expression Omnibus

630 **IC:** Input Control Library

631 **IHEC:** International Human Epigenetics Consortium

632 **IP:** Input Library

633 **KM:** Kaplan-Meier

634 **LogFC:** Log Fold-Change

635 **OCTANE:** Ontario-wide Cancer Targeted Nucleic Acid Evaluation

636 **OHS:** Ontario Healthy Study

637 **TCGA:** The Cancer Genome Atlas

638

639 Declarations

640 **Ethics approval and consent to participate**

641 Patient plasma samples were obtained from the Ontario Health Study (OHS) with protocols

642 approved by the University of Toronto Health Sciences research ethics board (protocol #34088).

643 All participants gave written informed consent prior to participation. All samples and participant

644 data were deidentified and assigned unique research IDs. Original OHS participant and CCO IDs
645 are not known to anyone outside the research group. Supplementary tables do not contain any
646 information that enables identification of the original participants.

647

648 **Availability of data and materials**

649 The datasets used and/or analysed during the current study are available from the corresponding
650 author on reasonable request.

651 **Competing interest statement**

652 DDC and SVB are listed as co-inventors on patents filed related to the cfMeDIP-seq technology.
653 SVB is co-inventor of a patent related to mutation-based ctDNA detection that is licensed to
654 Roche. DDC received research funds from Pfizer and Nektar therapeutics. DDC and SVB are co-
655 founders of, have ownership in, and serve in leadership roles at Adela. DWC has acted in a
656 consulting/advisory role for AstraZeneca, Exact Sciences, Eisai, Gilead, GlaxoSmithKline, Inivata,
657 Merck, Novartis, Pfizer and Roche, received research funding (to institution) from AstraZeneca,
658 Gilead, GlaxoSmithKline, Inivata, Merck, Pfizer, and Roche and holds a patent (US62/675,228)
659 for methods of treating cancers characterized by a high expression level of spindle and
660 kinetochore associated complex subunit 3 (ska3) gene. All the other authors declare no conflict
661 of interest.

662

663 **Funding**

664 OHS biological materials were stored at the Ontario Health Study Biobank, which is supported by
665 the Ontario Institute for Cancer Research through funding provided by the Government of Ontario,
666 the Princess Margaret Cancer Foundation, and a Genome Canada grant (OGI-136) to PA. The
667 OCTANE study was conducted with the support of the Ontario Institute for Cancer Research

668 through funding provided by the Government of Ontario and by the Princess Margaret Cancer
669 Foundation.

670

671 **Acknowledgments**

672 We would like to thank the Genomics Research Platform team at OICR for performing the
673 cfMeDIP-Seq assay on the plasma samples, as well as the insightful comments on the study from
674 members of the Ontario Institute for Cancer Research and Princess Margaret Cancer Centre. We
675 would also like to thank OCTANE investigators and study staff. Parts of the material are based
676 on data and information provided by Ontario Health, and includes data received by Ontario Health
677 from the Canadian Institute for Health Information (CIHI) and the Ministry of Health (MOH).
678 Funding was provided an Adaptive Oncology grant from the Ontario Ministry of Universities and
679 Colleges. The opinions, reviews, views and conclusions reported in this publication are those of
680 the authors and do not necessarily reflect those of Ontario Health, CIHI, and/or the MOH. No
681 endorsement by Ontario Health, CIHI, and/or the MOH is intended or should be inferred.

682

683 Author Information

684 **Authors and Affiliations**

685 **Computational Biology, Ontario Institute for Cancer Research, Toronto, Ontario, Canada**

686 Nicholas Cheng, Kimberly Skead, Tom Ouellette, David Soave, Philip Awadalla

687 **Department of Molecular Genetics, University of Toronto, Toronto, Ontario, Canada**

688 Nicholas Cheng, Kimberly Skead, Tom W. Ouellette, Philip Awadalla

689 **Department of Mathematics, Wilfrid Laurier University, Waterloo, Ontario, Canada**

690 David Soave

691 **Department of Medicine, University of Toronto, Toronto, Ontario, Canada**

692 Althaf Singhawansa, Mitchell Elliot, David W. Cescon

693 **Department of Medical Oncology, Princess Margaret Cancer Centre, University Health**
694 **Network, Toronto, Ontario, Canada**

695 Mitchell Elliot, David W. Cescon

696 **Department of Medical Biophysics, University of Toronto, Ontario, Canada**

697 Scott V. Bratman, Daniel D. De Carvalho

698 **Princess Margaret Cancer Centre, University Health Network, Toronto, Ontario, Canada**

699 Scott V. Bratman, David W. Cescon, Daniel D. De Carvalho

700 **Department of Radiation Oncology, University of Toronto, Toronto, Ontario, Canada**

701 Scott V. Bratman

702 **Ontario Health Study, Ontario Institute for Cancer Research, Toronto, Canada**

703 Philip Awadalla

704 **Dalla Lana School of Public Health, University of Toronto, Ontario Canada**

705 Philip Awadalla

706

707 **Author Contributions**

708 PA conceived the project. PA and KS are responsible for funding acquisition. KS performed
709 administrative linkage to identify incident cancer cases in the OHS. PA, NC and DS
710 conceptualized the project and study design. NC, PA and DS designed the computational and
711 statistical analyses. NC performed the bioinformatics, statistical analysis, figure generation and
712 manuscript writing. AS performed the bioinformatics for external validation samples. DWC and
713 SVB provided external validation data. PA, DS, SVB and DDC advised on the computational and
714 statistical analyses. PA, DS, SVB, DWC, KS, TWO wrote and revised the manuscript.

715

716 References

717 1. Siegel RL, Miller KD, Fuchs HE, Jemal A: **Cancer statistics, 2022**. CA: A Cancer Journal
718 for Clinicians 2022, **72**(1):7-33.

- 719 2. Smith RA, Andrews KS, Brooks D, Fedewa SA, Manassaram-Baptiste D, Saslow D,
720 Wender RC: **Cancer screening in the United States, 2019: A review of current**
721 **American Cancer Society guidelines and current issues in cancer screening.** CA: A
722 Cancer Journal for Clinicians 2019, **69**(3):184-210.
- 723 3. Ebell MH, Thai TN, Royalty KJ: **Cancer screening recommendations: an international**
724 **comparison of high income countries.** Public Health Rev 2018, **39**.
- 725 4. Brenner DR, Poirier A, Woods RR, Ellison LF, Billette J, Demers AA, Zhang SX, Yao C,
726 Finley C, Fitzgerald N, Saint-Jacques N, Shack L, Turner D, Holmes E, ,: **Projected**
727 **estimates of cancer in Canada in 2022.** CMAJ 2022, **194**(17):E601-E607.
- 728 5. Lehman CD, Arao RF, Sprague BL, Lee JM, Buist DSM, Kerlikowske K, Henderson LM,
729 Onega T, Tosteson ANA, Rauscher GH, Miglioretti DL: **National Performance**
730 **Benchmarks for Modern Screening Digital Mammography: Update from the Breast**
731 **Cancer Surveillance Consortium.** Radiology 2017, **283**(1):49-58.
- 732 6. Guertin M, Théberge I, Zomahoun HTV, Dufresne M, Pelletier É, Brisson J:
733 **Mammography Clinical Image Quality and the False Positive Rate in a Canadian**
734 **Breast Cancer Screening Program.** Can Assoc Radiol J 2018, **69**(2):169-175.
- 735 7. Klarenbach S, Sims-Jones N, Lewin G, Singh H, Thériault G, Tonelli M, Doull M, Courage
736 S, Garcia AJ, Thombs BD, ,: **Recommendations on screening for breast cancer in**
737 **women aged 40–74 years who are not at increased risk for breast cancer.** CMAJ
738 2018, **190**(49):E1441-E1451.
- 739 8. Cescon DW, Bratman SV, Chan SM, Siu LL: **Circulating tumor DNA and liquid biopsy**
740 **in oncology.** Nat Cancer 2020, **1**(3):276-290.
- 741 9. Shen SY, Singhanian R, Fehringer G, Chakravarthy A, Roehrl MHA, Chadwick D, Zuzarte
742 PC, Borgida A, Wang TT, Li T, Kis O, Zhao Z, Spreafico A, Medina TdS, Wang Y, Roulois
743 D, Ettayebi I, Chen Z, Chow S, Murphy T, Arruda A, O’Kane GM, Liu J, Mansour M,
744 McPherson JD, O’Brien C, Leighl N, Bedard PL, Fleshner N, Liu G, Minden MD, Gallinger

- 745 S, Goldenberg A, Pugh TJ, Hoffman MM, Bratman SV, Hung RJ, Carvalho DDD:
746 **Sensitive tumour detection and classification using plasma cell-free DNA**
747 **methylomes**. Nature 2018, **563**(7732):579-583.
- 748 10. Liu MC, Oxnard GR, Klein EA, Swanton C, Seiden MV, CCGA Consortium: **Sensitive**
749 **and specific multi-cancer detection and localization using methylation signatures**
750 **in cell-free DNA**. Ann Oncol 2020, **31**(6):745-759.
- 751 11. Cohen JD, Li L, Wang Y, Thoburn C, Afsari B, Danilova L, Douville C, Javed AA, Wong
752 F, Mattox A, Hruban RH, Wolfgang CL, Goggins MG, Dal Molin M, Wang T, Roden R,
753 Klein AP, Ptak J, Dobbyn L, Schaefer J, Silliman N, Popoli M, Vogelstein JT, Browne JD,
754 Schoen RE, Brand RE, Tie J, Gibbs P, Wong H, Mansfield AS, Jen J, Hanash SM, Falconi
755 M, Allen PJ, Zhou S, Bettegowda C, Diaz LA, Tomasetti C, Kinzler KW, Vogelstein B,
756 Lennon AM, Papadopoulos N: **Detection and localization of surgically resectable**
757 **cancers with a multi-analyte blood test**. Science 2018, **359**(6378):926-930.
- 758 12. Jamshidi A, Liu MC, Klein EA, Venn O, Hubbell E, Beausang JF, Gross S, Melton C, Fields
759 AP, Liu Q, Zhang N, Fung ET, Kurtzman KN, Amini H, Betts C, Civello D, Freese P, Calef
760 R, Davydov K, Fayzullina S, Hou C, Jiang R, Jung B, Tang S, Demas V, Newman J, Sakarya
761 O, Scott E, Shenoy A, Shojaee S, Steffen KK, Nicula V, Chien TC, Bagaria S, Hunkapiller
762 N, Desai M, Dong Z, Richards DA, Yeatman TJ, Cohn AL, Thiel DD, Berry DA, Tummala
763 MK, McIntyre K, Sekeres MA, Bryce A, Aravanis AM, Seiden MV, Swanton C: **Evaluation**
764 **of cell-free DNA approaches for multi-cancer early detection**. Cancer Cell 2022, .
- 765 13. Liu J, Zhao H, Huang Y, Xu S, Zhou Y, Zhang W, Li J, Ming Y, Wang X, Zhao S, Li K,
766 Dong X, Ma Y, Qian T, Chen X, Xing Z, Zhang Y, Chen H, Liu Z, Pang D, Zhou M, Wu Z,
767 Wang X, Wang X, Wu N, Su J: **Genome-wide cell-free DNA methylation analyses**
768 **improve accuracy of non-invasive diagnostic imaging for early-stage breast cancer**.
769 Molecular Cancer 2021, **20**(1):36.

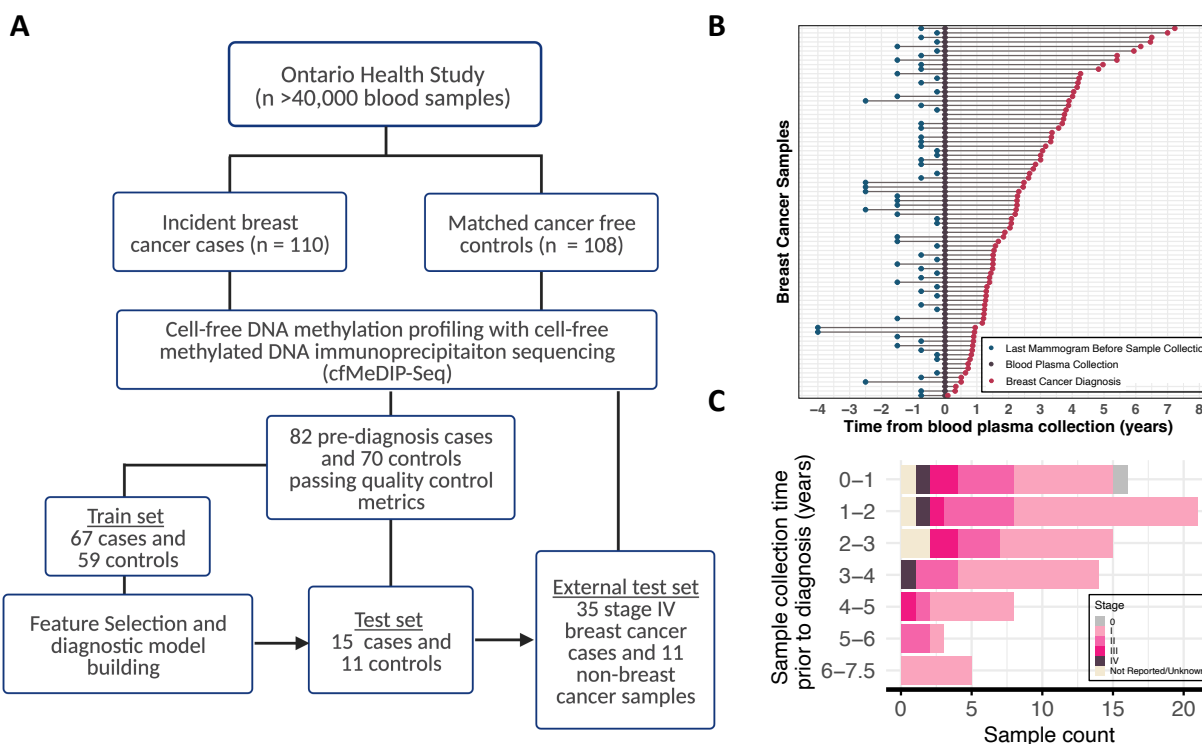
- 770 14. Zhang X, Zhao D, Yin Y, Yang T, You Z, Li D, Chen Y, Jiang Y, Xu S, Geng J, Zhao Y, Wang
771 J, Li H, Tao J, Lei S, Jiang Z, Chen Z, Yu S, Fan J, Pang D: **Circulating cell-free DNA-**
772 **based methylation patterns for breast cancer diagnosis.** npj Breast Cancer 2021,
773 7(1):106.
- 774 15. Cristall K, Bidard F, Pierga J, Rauh MJ, Popova T, Sebbag C, Lantz O, Stern M, Mueller CR:
775 **A DNA methylation-based liquid biopsy for triple-negative breast cancer.** npj Precision
776 Oncology 2021, 5(1):53.
- 777 16. Moss J, Zick A, Grinshpun A, Carmon E, Maoz M, Ochana BL, Abraham O, Arieli O,
778 Germansky L, Meir K, Glaser B, Shemer R, Uziely B, Dor Y: **Circulating breast-derived**
779 **DNA allows universal detection and monitoring of localized breast cancer.** Annals
780 of Oncology 2020, 31(3):395-403.
- 781 17. Kirsh VA, Skead K, McDonald K, Kreiger N, Little J, Menard K, McLaughlin J, Mukherjee
782 S, Palmer LJ, Goel V, Purdue MP, Awadalla P: **Cohort Profile: The Ontario Health**
783 **Study (OHS).** Int J Epidemiol 2022, :dyac156.
- 784 18. Malone ER, Saleh RR, Yu C, Ahmed L, Pugh T, Torchia J, Bartlett J, Virtanen C, Hotte
785 SJ, Hilton J, Welch S, Robinson A, McCready E, Lo B, Sadikovic B, Feilotter H, Hanna
786 TP, Kamel-Reid S, Stockley TL, Siu LL, Bedard PL: **OCTANE (Ontario-wide Cancer**
787 **Targeted Nucleic Acid Evaluation): a platform for intraprovincial, national, and**
788 **international clinical data-sharing.** Curr Oncol 2019, 26(5):e618-e623.
- 789 19. Shen SY, Burgener JM, Bratman SV, Carvalho DDD: **Preparation of cfMeDIP-seq**
790 **libraries for methylome profiling of plasma cell-free DNA.** Nature Protocols 2019,
791 14(10):2749-2780.
- 792 20. Mohn F, Weber M, Schübeler D, Roloff T: **Methylated DNA immunoprecipitation**
793 **(MeDIP).** Methods Mol Biol 2009, 507:55-64.

- 794 21. Smith T, Heger A, Sudbery I: **UMI-tools: modeling sequencing errors in Unique**
795 **Molecular Identifiers to improve quantification accuracy.** *Genome Res* 2017,
796 **27(3):491-499.**
- 797 22. Langmead B, Salzberg SL: **Fast-gapped read alignment with Bowtie 2.** *Nature methods*
798 2012, **9(4):357-359.**
- 799 23. Li, H. *et al.* The Sequence Alignment/Map format and SAMtools. *Bioinformatics* **25**, 2078-
800 2079 (2009).
- 801 24. Burgener JM, Zou J, Zhao Z, Zheng Y, Shen SY, Huang SH, Keshavarzi S, Xu W, Liu FF,
802 Liu G, Waldron JN, Weinreb I, Spreafico A, Siu LL, de Almeida JR, Goldstein DP, Hoffman
803 MM, De Carvalho DD, Bratman SV: **Tumor-Naïve Multimodal Profiling of Circulating**
804 **Tumor DNA in Head and Neck Squamous Cell Carcinoma.** *Clin Cancer Res* 2021,
805 **27(15):4230-4244.**
- 806 25. Lienhard M, Grimm C, Morkel M, Herwig R, Chavez L: **MEDIPS: genome-wide**
807 **differential coverage analysis of sequencing data derived from DNA enrichment**
808 **experiments.** *Bioinformatics* 2014, **30(2):284-286.**
- 809 26. Love MI, Huber W, Anders S: **Moderated estimation of fold change and dispersion for**
810 **RNA-seq data with DESeq2.** *Genome Biol* 2014, **15(12):550.**
- 811 27. Stunnenberg HG, et. al: **The International Human Epigenome Consortium: A**
812 **Blueprint for Scientific Collaboration and Discovery.** *Cell* 2016, **167(5):1145-1149.**
- 813 28. Noguchi S, et. al: **FANTOM5 CAGE profiles of human and mouse samples.** *Scientific*
814 *data* 2017, **4(1):170112.**
- 815 29. Teschendorff AE: **Avoiding common pitfalls in machine learning omic data science.**
816 *Nature Materials* 2019, **18(5):422-427.**
- 817 30. Teschendorff AE, Jones A, Fiegl H, Sargent A, Zhuang JJ, Kitchener HC, Widschwendter
818 M: **Epigenetic variability in cells of normal cytology is associated with the risk of**
819 **future morphological transformation.** *Genome Med* 2012, **4(3):24.**

- 820 31. Kuhn M: **Building Predictive Models in R Using the caret Package**. Journal of
821 Statistical Software 2008, **28**(1):1-26.
- 822 32. Beleites C, Baumgartner R, Bowman C, Somorjai R, Steiner G, Salzer R, Sowa MG:
823 **Variance reduction in estimating classification error using sparse datasets**.
824 Chemometrics and Intelligent Laboratory Systems 2005, **79**(1):91-100.
- 825 33. Harrell FE, Califf RM, Pryor DB, Lee KL, Rosati RA: **Evaluating the yield of medical**
826 **tests**. JAMA 1982, **247**(18):2543-2546.
- 827 34. Heagerty PJ, Lumley T, Pepe MS: **Time-dependent ROC curves for censored survival**
828 **data and a diagnostic marker**. Biometrics 2000, **56**(2):337-344.
- 829 35. Aryee MJ, Jaffe AE, Corrada-Bravo H, Ladd-Acosta C, Feinberg AP, Hansen KD, Irizarry
830 RA: **Minfi: a flexible and comprehensive Bioconductor package for the analysis of**
831 **Infinium DNA methylation microarrays**. Bioinformatics 2014, **30**(10):1363-1369.
- 832 36. Hansen KD, Timp W, Bravo HC, Sabunciyan S, Langmead B, McDonald OG, Wen B, Wu
833 H, Liu Y, Diep D, Briem E, Zhang K, Irizarry RA, Feinberg AP: **Increased methylation**
834 **variation in epigenetic domains across cancer types**. Nat Genet 2011, **43**(8):768-775.
- 835 37. Teschendorff AE, Jones A, Fiegler H, Sargent A, Zhuang JJ, Kitchener HC, Widschwendter
836 M: **Epigenetic variability in cells of normal cytology is associated with the risk of**
837 **future morphological transformation**. Genome Med 2012, **4**(3):24.
- 838 38. Esteller M: **Epigenetic gene silencing in cancer: the DNA hypermethylome**. Hum Mol
839 Genet 2007, **16**(R1):R50-R59.
- 840 39. Sasaki Y, Tamura M, Takeda K, Ogi K, Nakagaki T, Koyama R, Idogawa M, Hiratsuka H,
841 Tokino T: **Identification and characterization of the intercellular adhesion molecule-2**
842 **gene as a novel p53 target**. Oncotarget 2016, **7**(38):61426-61437.
- 843 40. Chen S, Petricca J, Ye W, Guan J, Zeng Y, Cheng N, Gong L, Shen SY, Hua JT, Crumbaker
844 M, Fraser M, Liu S, Bratman SV, van der Kwast T, Pugh T, Joshua AM, De Carvalho DD,
845 Chi KN, Awadalla P, Ji G, Feng F, Wyatt AW, He HH: **The cell-free DNA methylome**

- 846 **captures distinctions between localized and metastatic prostate tumors.** Nature
847 Communications 2022, **13**(1):6467.
- 848 41. Widschwendter M, Evans I, Jones A, Ghazali S, Reisel D, Ryan A, Gentry-Maharaj A, Zikan
849 M, Cibula D, Eichner J, Alunni-Fabbroni M, Koch J, Janni WJ, Paprotka T, Wittenberger T,
850 Menon U, Wahl B, Rack B, Lempiäinen H: **Methylation patterns in serum DNA for early**
851 **identification of disseminated breast cancer.** Genome Medicine 2017, **9**(1):115.
- 852 42. Liu MC, Maddala T, Aravanis A, Hubbell E, Beausang JF, Filippova D, Gross S, Jamshidi A,
853 Kurtzman K, Shen L, Valouev A, Venn O, Zhang N, Smith DA, Couch F, Curtis C, Williams
854 RT, Klein EA, Hartman A, Baselga J: **Breast cancer cell-free DNA (cfDNA) profiles reflect**
855 **underlying tumor biology: The Circulating Cell-Free Genome Atlas (CCGA) study.** JCO
856 2018, **36**(15):536.
- 857 43. Sonesson C, Gerster S, Delorenzi M: **Batch Effect Confounding Leads to Strong Bias in**
858 **Performance Estimates Obtained by Cross-Validation.** PloS one 2014, **9**(6):e100335.
- 859 44. Ontario Health. **The Ontario Cancer Screening Performance Report 2020.** Cancer Care
860 Ontario. 2020.
- 861 45. Boice JD, Harvey EB, Blettner M, Stovall M, Flannery JT: **Cancer in the Contralateral**
862 **Breast after Radiotherapy for Breast Cancer.** New England Journal of Medicine 1992,
863 **326**(12):781-785.
- 864

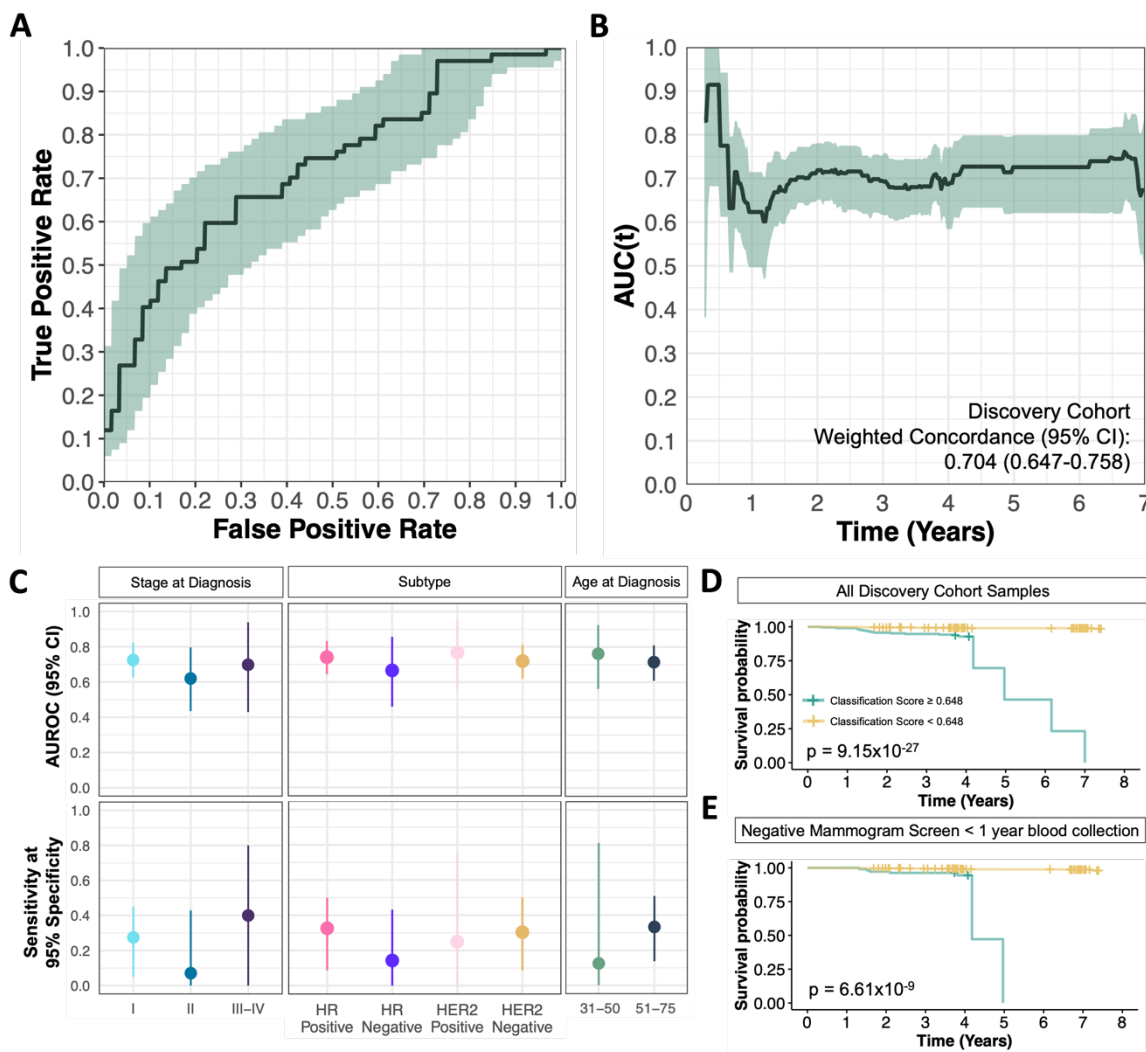
865



866 **Fig. 1: Overview of study design and incident breast cancer cases in the Ontario Healthy**
 867 **Study.**

868 **(A)** Outline of participant recruitment and blood plasma sample selection process in the Ontario
 869 Health Study (OHS). Cell-free DNA methylome of blood plasma from 218 OHS participants
 870 profiled with cell-free methylation DNA immunoprecipitation sequencing (cfMeDIP-Seq). 152
 871 samples passed all quality control metrics. Train set of 67 pre-diagnosis breast cancer cases and
 872 59 cancer-free controls were used to identify differentially methylated regions for building breast
 873 cancer diagnostic classifiers. Held-out batch of 15 pre-diagnosis breast cancer cases and 11
 874 cancer-free controls used to evaluate diagnostic classifier predictive performance. External test
 875 set of 35 breast cancer samples collected at diagnosis time and 11 non-breast cancer samples
 876 were used to further validate diagnostic classifier performance. **(B)** Timeline of blood plasma
 877 collection, breast cancer diagnosis and last mammogram prior to biologic collection across

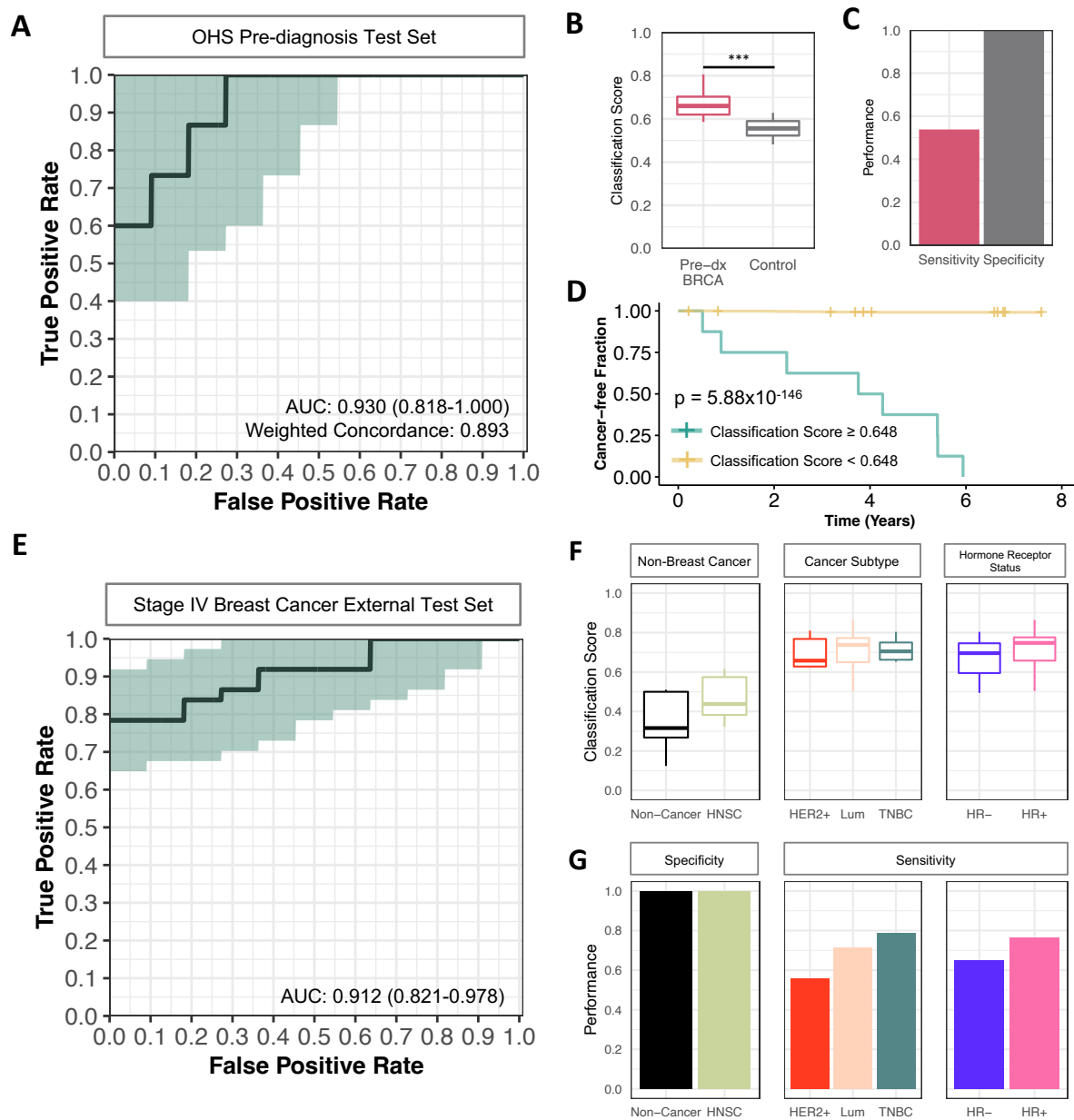
878 incident breast cancer cases in OHS **(C)** Pre-diagnosis OHS cases across time between sample
 879 collection and breast cancer diagnosis. Colors indicate stage at diagnosis across cases.



880
 881 **Fig. 2: Classification performance of discovery set OHS pre-diagnosis cases and controls**
 882 **using top 150 hypermethylated regions.**

883 Test-fold classification scores averaged across 100 repeats for each sample. **(A)** Bootstrapped
 884 receiver operating characteristic (ROC) curves of discovery cohort sample classification scores.
 885 Mean performance across 1000 bootstraps are shown in black, with 95% confidence intervals
 886 indicated by shaded green regions. **(B)** Time-dependent area under ROC curves (AUC(t))
 887 weighted for the true cumulative age-specific breast cancer incidence rates in Canada. Mean

888 AUC(t) shown in black lines, with shaded regions indicating 95% confidence intervals **(C)**
889 Bootstrap AUROC and sensitivity at 95% specificity for classifying discovery cohort stratified by
890 subtype at diagnosis, stage at diagnosis, and age at diagnosis. Dots show mean performance,
891 while lines indicate 95% confidence intervals **(D&E)** Kaplan-Meier curves indicating cancer-free
892 survival time following blood collection across **(D)** all samples and **(E)** in samples with a negative
893 screening mammogram within one year of blood collection. Samples are stratified by mean
894 classification score above or below 0.648.



895

896

897 **Fig. 3: Classification performance of independent validation set pre-diagnosis and late-**
 898 **stage breast cancer cases and controls.**

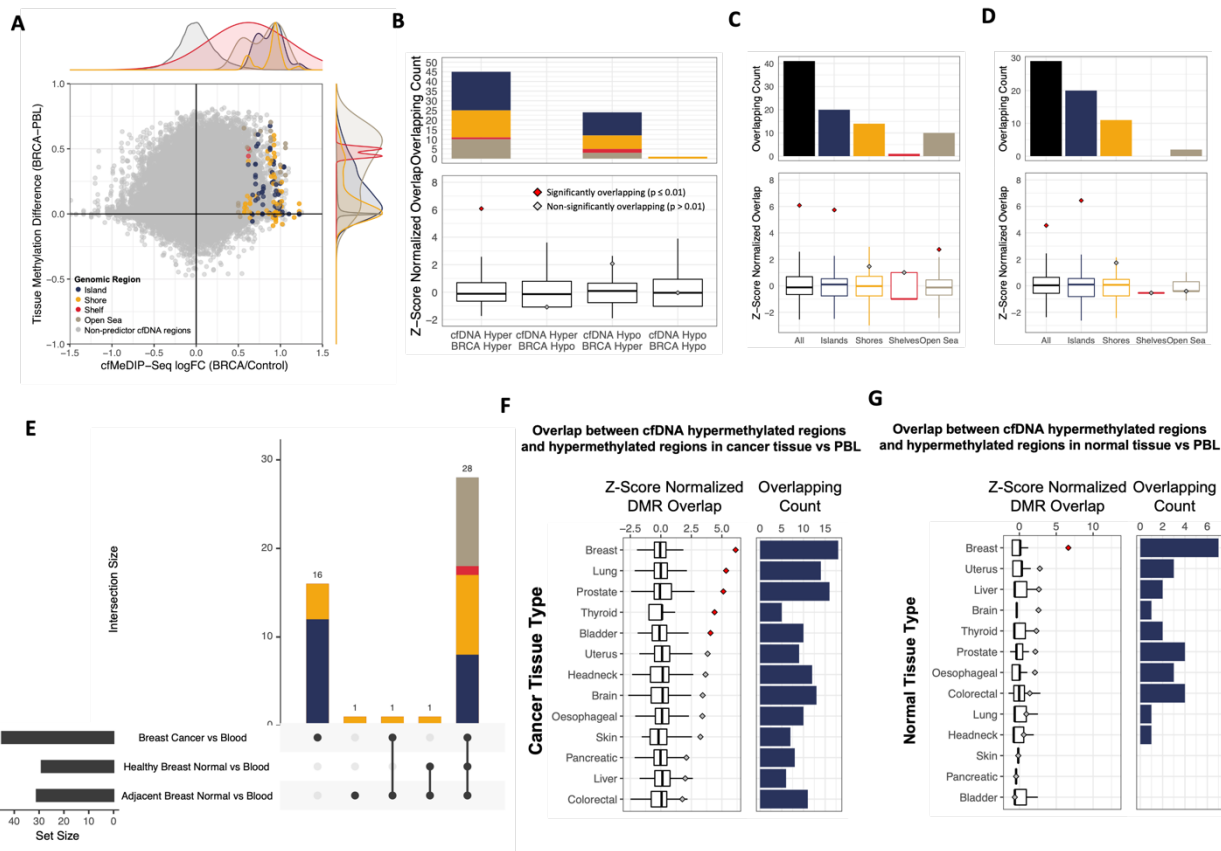
899 **(A)** ROC for classifying test set pre-diagnosis breast cancer cases (n = 15) and controls (n = 11)

900 from a separate batch of OHS samples. Predictive performance of classifier trained using top 150

901 ranked hypermethylated regions identified from discovery cohort samples **(B)** Predicted

902 classification score among OHS test set pre-diagnosis cases and controls ($p = 4.10 \times 10^{-5}$) and **(C)**
903 corresponding sensitivity and specificity using a classification cut off of 0.648 previously
904 determined from discovery cohort samples. **(D)** Kaplan-Meier survival curves of pre-diagnosis test
905 set samples grouped by classification score cut off above (green) or below (yellow) 0.648 (log-
906 rank test $p = 5.88 \times 10^{-146}$). Cut off determined from discovery cohort samples that yielded 95%
907 specificity. **(E)** ROC for classifying all external test set of metastatic breast cancer cases collected
908 at the time of diagnosis ($n = 35$) cases and non-breast cancer controls ($n = 11$). External samples
909 were classified by the diagnostic model built from discovery cohort samples. Samples from breast
910 cancer cases were collected at the time of breast cancer diagnosis before treatment **(F&G)**
911 External test set classification scores across non-cancer controls ($n = 5$), head and neck
912 squamous cell carcinomas ($n = 6$) cases, and late-stage breast cancer ($n = 35$) samples. **(F)**
913 Classification scores of external test set samples from diagnostic classifier stratified by non-breast
914 cancer samples, PAM50 and hormone receptor subtype **(G)** Specificity and sensitivity across
915 breast cancer subgroups for classifying external test set samples using cut-off score of 0.648 to
916 discriminate breast cancer cases from controls.

917



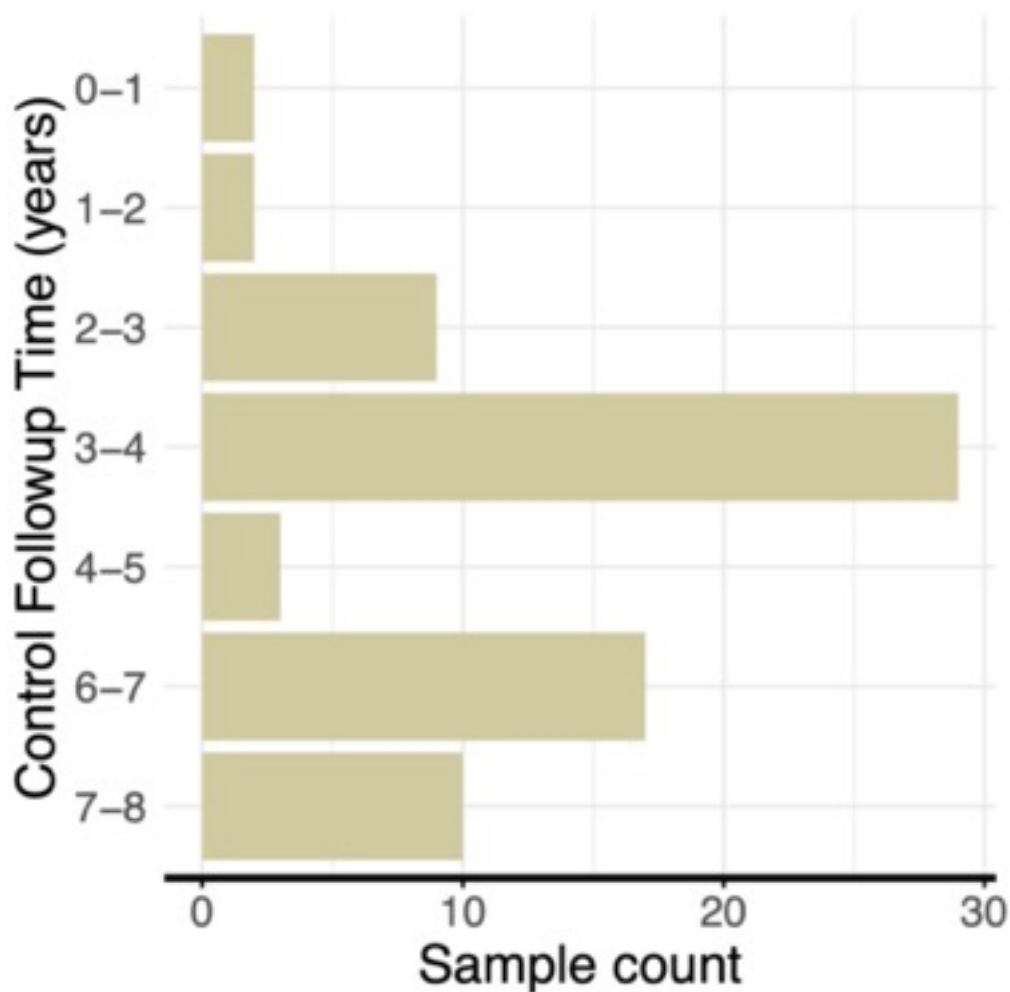
918

919 **Fig. 4: Overlap between top 150 pre-diagnosis breast cancer cfDNA hypermethylated**
 920 **regions and bulk tissue hypermethylated regions**

921 **(A)** Association between the log fold-change in cfMeDIP-Seq cfDNA methylation of discovery set
 922 pre-diagnosis cases versus controls and difference in 450k array beta methylation level between
 923 bulk breast cancer tissue versus PBLs. Each point represents a cfDNA region overlapping a 450k
 924 methylation array CpG Site. Gray dots represent background cfDNA regions, while non-grey
 925 colored points represent CpG sites in 75 out of the top 150 differentially hypermethylated regions
 926 in pre-diagnosis cfDNA colored by CpG islands (blue), shores (yellow), shelves (red) or open sea
 927 (brown) regions. **(B)** Number of overlapping regions between the top 150 pre-diagnosis breast
 928 cancer cfDNA DMRs, and significant DMRs in 450k methylation array bulk breast cancer tissue
 929 relative to peripheral blood leukocytes (PBLs) ($p < 0.0001$ & absolute difference > 0.1). Top bar

930 plots are colored by CpG islands (blue), shores (yellow), shelves (red) or open sea (brown)
931 regions. Points in the plot below shows the observed z-score normalised overlapping count
932 compared to the boxplots showing the distribution of overlapping counts between bulk breast
933 tissue vs blood DMRs and random cfDNA background regions across 3000 permutations. Red
934 points indicate significant overlap ($p \leq 0.01$) in hypermethylated regions, while gray points indicate
935 non-significant overlap ($p > 0.01$). **(C-D)** Overlap between the top 150 significantly
936 hypermethylated pre-diagnosis cfDNA regions and significantly hypermethylated regions in **(C)**
937 bulk breast cancer tissue versus blood, and **(D)** bulk breast cancer versus adjacent breast normal
938 tissue. Boxplots represent distribution of overlap between significantly hypermethylated bulk
939 breast cancer tissue markers and background cfDNA regions. **(E)** Intersecting regions
940 significantly hypermethylated in bulk cancer, adjacent normal and healthy normal breast tissue
941 relative to PBLs that overlap with 75 out of the top 150 cfDNA hypermethylated regions. **(F-G)**
942 Overlap between 75 out of the top 150 hypermethylated pre-diagnosis cfDNA regions located in
943 CpG islands and significantly hypermethylated regions
944
945

Fig. S1



946

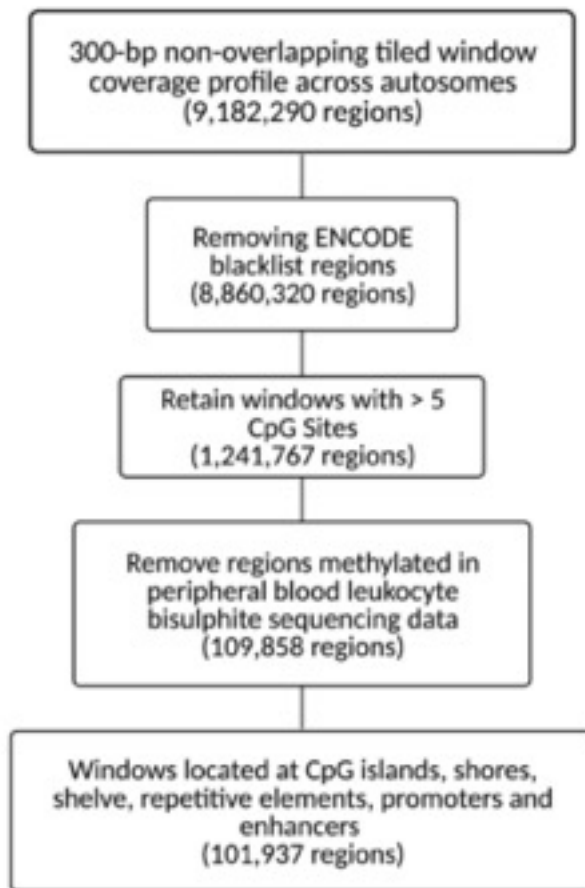
947 **Fig. S1: Matched cancer-free control sample follow-up time** Selected control plasma (n = 70)

948 were matched to cases by sex, age, time of sample collection, smoking status and alcohol

949 consumption frequency.

950

Fig. S2



951

952 **Fig. S2: Flowchart of filters applied to reduce background regions methylated and enrich**

953 **for DMRs associated with breast cancer.** Flowchart of filters applied to reduce background

954 regions methylated in peripheral blood leukocytes and enrich for DMRs associated with breast

955 cancer development. Feature search space started with genome-wide coverage profiles across

956 9,182,290 300-bp nonoverlapping tiled windows. To reduce background signals derived from

957 peripheral blood cells (PBLs) and enrich for tumour-derived signals, regions frequently methylated

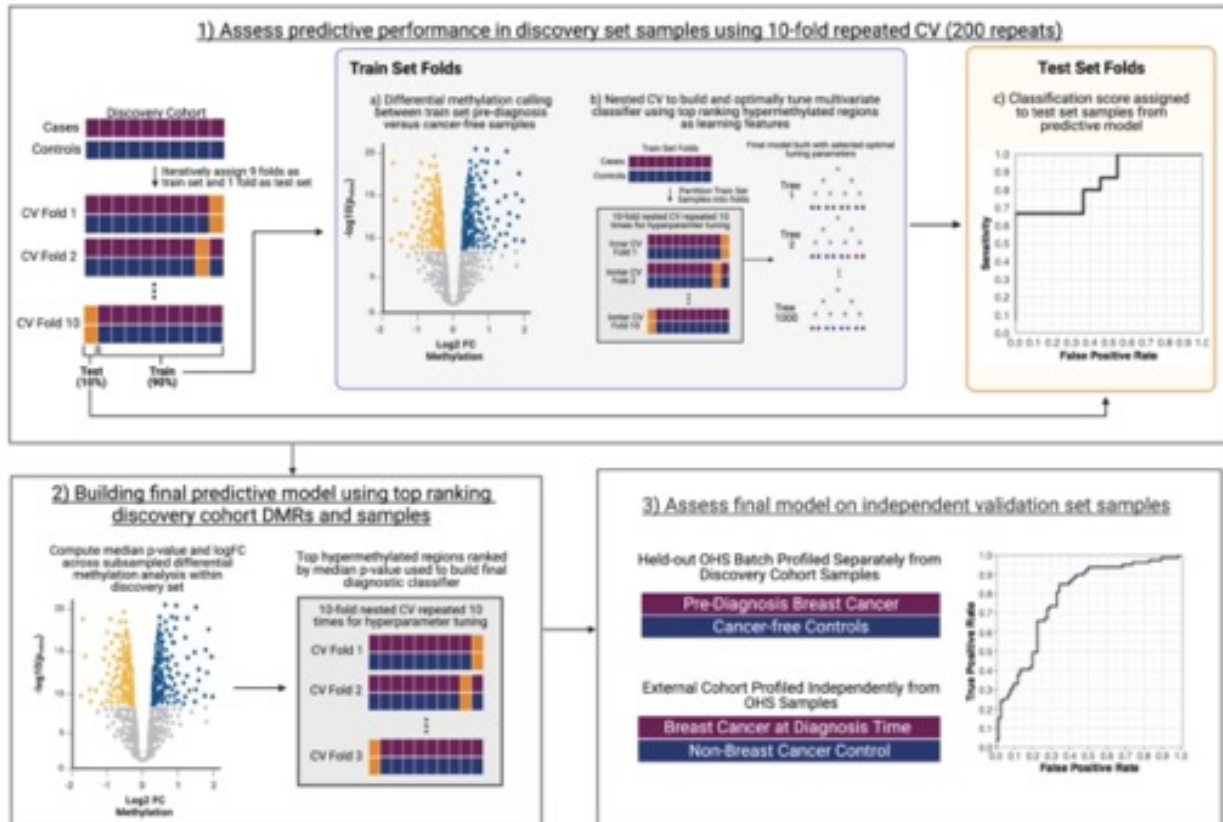
958 in PBLs (average methylation across 300 base pair window of over 0.25) whole-genome bisulfite

959 sequencing data from IHEC were filtered out (n = 79). To enrich for CpG dense and regulatory

960 regions, windows with at least six or more CpG sites, and located at CpG islands, shores, shelves,

961 repeat elements, and FANTOM5 enhancers or promoters were selected, leaving 101,937 regions
 962 remaining to perform differential methylation analysis.
 963

Fig. S3



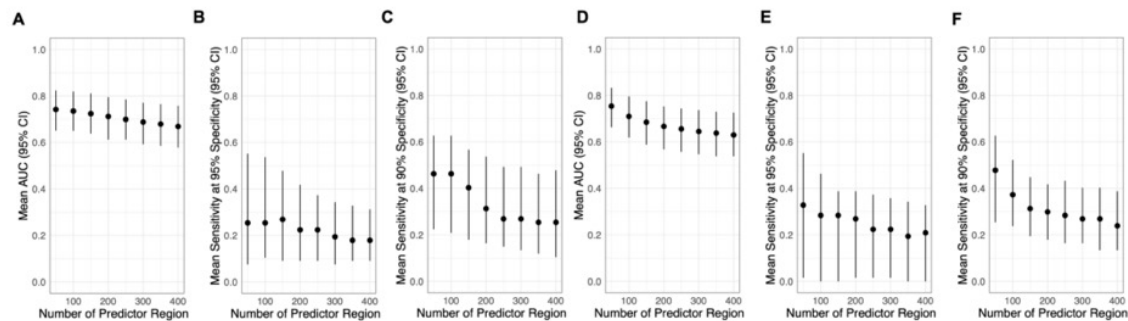
964
 965 **Fig. S3: Schematic of the analytical approach performed to assess predictive performance**
 966 **of pre-diagnosis cfDNA methylation profiles.** To assess predictive performance in discovery
 967 cohort samples and identify optimal number of features to use in the final classifier, a 10-fold CV
 968 repeated 100 times was performed on the discovery set. Pre-diagnosis breast cancer cases and
 969 controls were partitioned into 10-fold splits, splitting the number of cases by years prior to
 970 diagnosis evenly among each fold. Iteratively, nine-folds were selected as train set samples and
 971 used to perform differential methylation calling to identify and rank the top hypermethylated
 972 regions in pre-diagnosis breast cancer cfDNA. The top ranking hypermethylated regions among

973 pre-diagnosis cases in the 9-folds are used to build a random forest diagnostic classifier to
974 discriminate individuals with undetected breast cancers. Samples in the one remaining held-out
975 test fold that was not involved in any aspect of feature selection or model building were assigned
976 a classification score from the model built using nine train folds to evaluate the classifier
977 performance. This process was iteratively repeated 10 times, such that each fold was the held-
978 out test fold once. We repeated this 10-fold CV split strategy 100 times, each time with random
979 sample partitioning into folds to infer the overall performance in discovery cohort samples. Across
980 the 100 repeats, differential methylation calling was performed 1000 times (10 times per CV
981 repeat) with different subsampled cases and controls. The mean logFC in methylation and p-
982 value was computed for each region, and ranked according to p-value. The top 150
983 hypermethylated regions were used to build diagnostic classifiers trained with all discovery cohort
984 samples, using a 10-fold nested CV repeated 10 times for hyperparameter tuning. The classifier
985 performance was evaluated on independent test set samples consisting of a held-out batch of
986 pre-diagnosis cases and controls from OHS and stage IV breast cancers collected at the time of
987 diagnosis and controls from external cohorts.
988

989

990

Fig. S4



991

992 **Fig. S4: Discovery cohort test-fold performance across varying number of top ranking**

993 **regions.** Across the 100 repeated 10-fold cross validation, the top hypermethylated features

994 identified from train set folds were ranked according to p-values calculated by performing (A-C) a

995 Wald's test of the negative binomial regression coefficient between pre-diagnosis cases and

996 controls and (D-F) a Bartlett's test for variability between pre-diagnosis cases and controls within

997 each 10-fold CV repeat. Diagnostic classifiers built using the top ranking features in train set folds

998 were assessed on held-out test folds by assigning classification scores. Average test-fold

999 classification scores were computed for each sample across the 100 repeats. Averaged risk

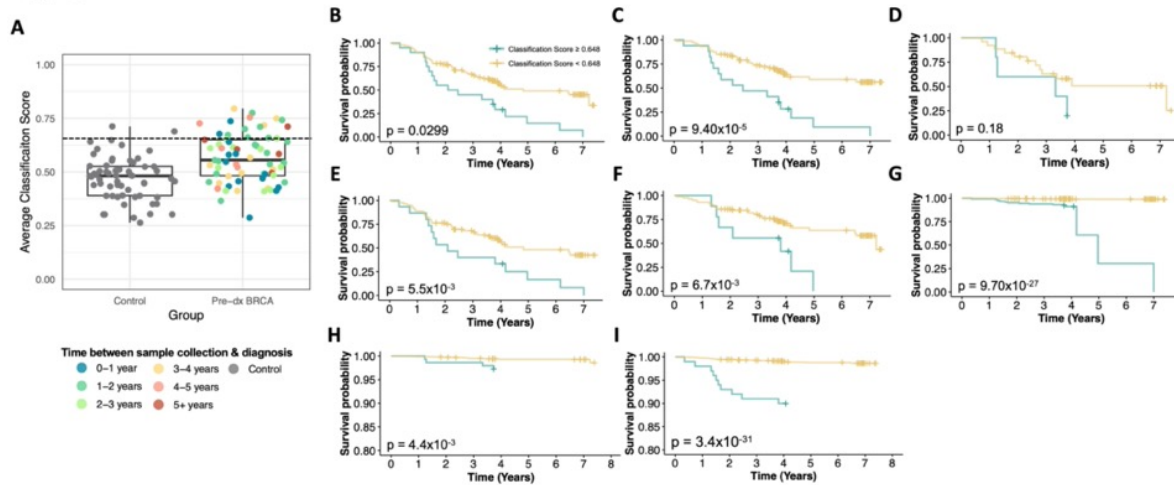
1000 scores were bootstrapped 1000 times to obtain (A & D) mean AUROC, (B & E) mean sensitivity

1001 at 95% specificity and (C & F) sensitivity at 90% specificity. Dots indicate mean performance and

1002 lines represent 95% percent confidence intervals.

1003

Fig. S5



1004

1005 **Fig. S5: Kaplan-Meier survival curves of discovery set samples stratified by mean test-fold**

1006 **classification scores (A)** Average classification scores for controls and pre-diagnosis breast

1007 cancer (BRCA) cases in the discovery cohort. Mean classification scores were calculated by

1008 averaging all test-fold classification score across repeats per sample. Each dot represents a

1009 sample colored by the time between sample collection and diagnosis for cases and grey for

1010 controls. Dotted line indicates classification score (0.648) yielding 95% specificity. **(B-F)**

1011 Unweighted Kaplan-Meier survival curves stratified by discovery cohort samples above and below

1012 a mean classification score of 0.648 for controls and **(B)** all cases, **(C)** hormone receptor positive

1013 cases, **(D)** cases diagnosed between ages 31-50, **(E)** cases diagnosed between ages 51-75, and

1014 **(F)** cases with a negative mammogram screen within one year of diagnosis. **(G-I)** Kaplan-Meier

1015 survival curves weighted by age specific cumulative breast cancer incidence rates from the

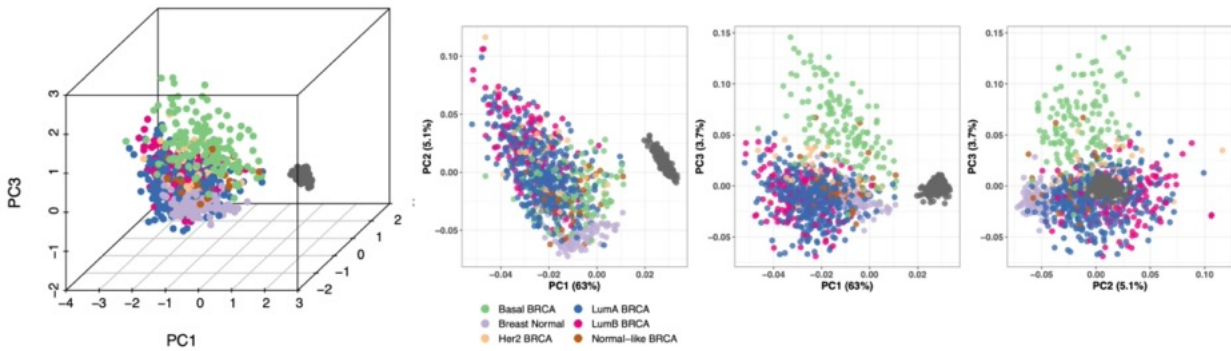
1016 Canadian Cancer Registry stratifying controls and **(G)** hormone receptor positive cases, **(H)** cases

1017 diagnosed at ages 31-50, and **(I)** cases diagnosed at ages 51-75.

1018

1019

Fig. S6

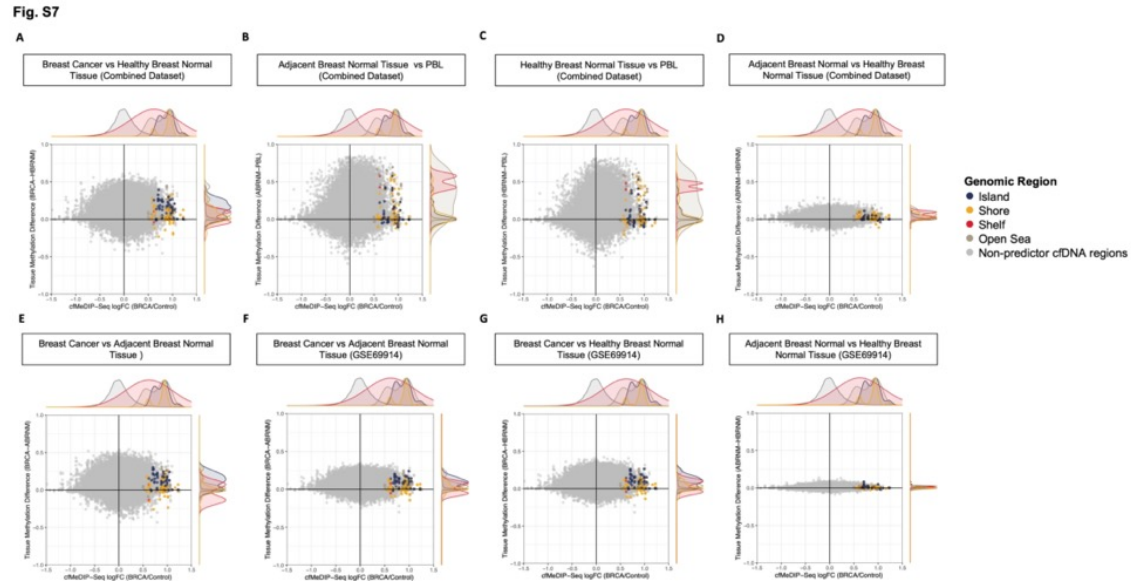


1020

1021 **Fig. S6: Pre-diagnosis cfDNA methylation signatures discriminates bulk breast cancer.**

1022 Principal component analysis of TCGA 450k methylation array of bulk breast cancer tissue (n =
1023 787), bulk normal breast tissue (n = 97) and peripheral blood leukocytes (n = 628) across 156
1024 CpG sites overlapping the 75 out of the top 150 hypermethylated regions in pre-diagnosis breast
1025 cancer cfDNA that contain at least one CpG site profiled by the 450k methylation array.

1026



1027

1028 **Fig. S7: Association between cfDNA methylation and in bulk breast tissue methylation**

1029 **profiles. (A-E)** Log-fold change in cfDNA methylation between cases and controls in background

1030 (grey) and in 75 regions out of the top 150 hypermethylated (colored) regions identified from

1031 discovery cohort pre-diagnosis breast cancers targeted by the 450k DNA methylation array

1032 compared to the absolute change in methylation in overlapping sites between bulk **(A)** breast

1033 cancer (BRCA) tissue vs healthy breast tissue (HBRNM), **(B)** adjacent breast normal tissue

1034 (ABRNM) vs peripheral blood leukocytes (PBL), **(C)** HBRNM vs PBLs, **(D)** ABRNM vs HBRNM,

1035 and **(E)** BRCA vs ABRNM in combined 450k methylation array datasets (GSE133985,

1036 GSE74214, GSE88883, GSE66313 & GSE101961). **(F-H)** Log-fold change in methylation in

1037 cfDNA compared to the absolute change in methylation among overlapping CpG sites between

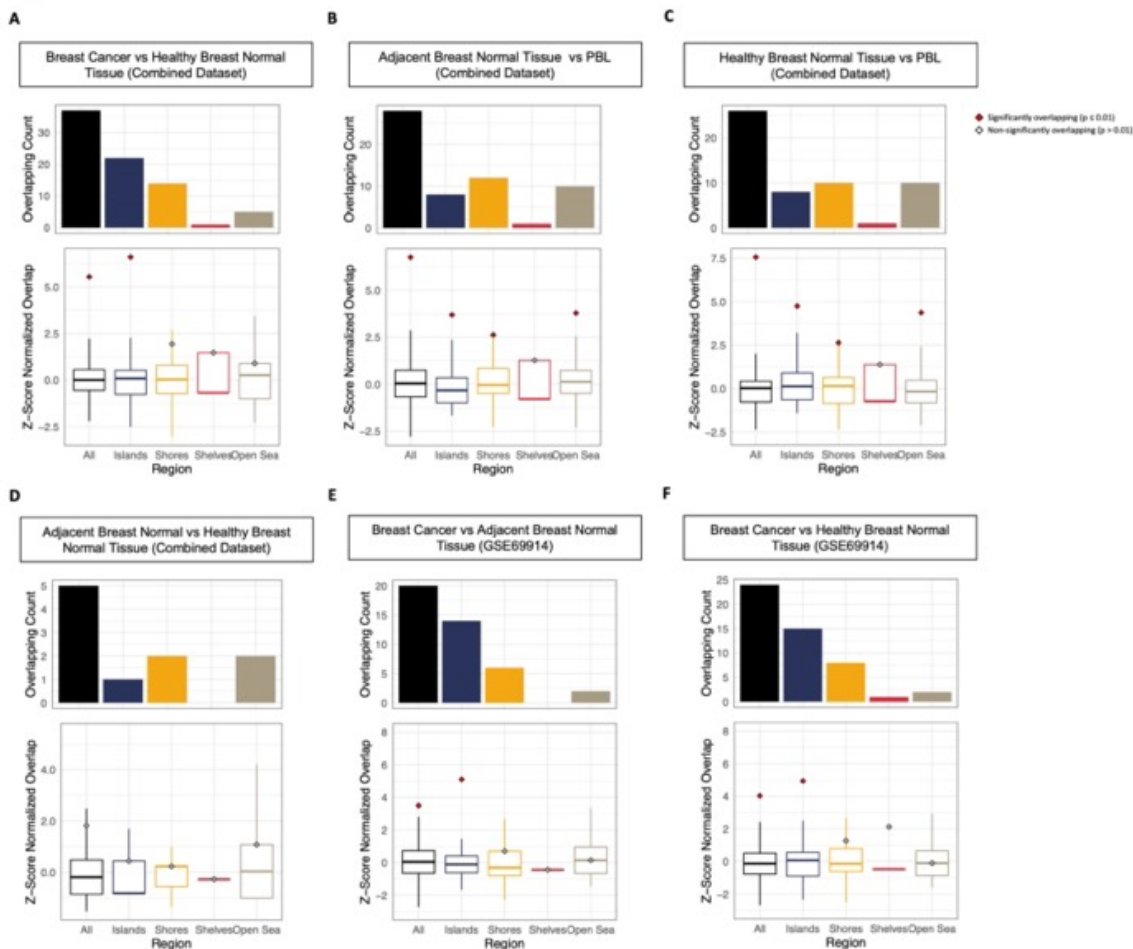
1038 **(F)** BRCA vs ABRNM, **(G)** BRCA vs HBNM and **(H)** ABRNM vs HBRNM in 450k methylation array

1039 data from GSE69914. Each point represents a CpG site on the 450k methylation array and colors

1040 indicate the genomic region the CpG site is located for predictor regions.

1041

Fig. S8

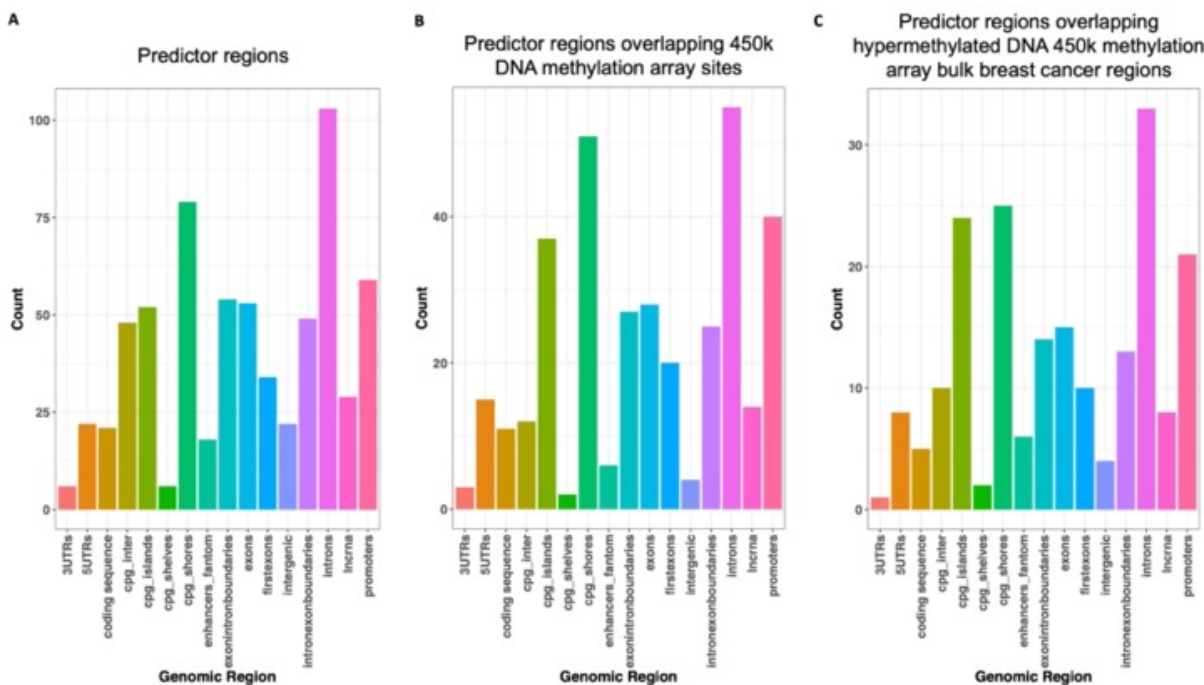


1042

1043 **Fig. S8: Overlapping hypermethylated regions between pre-diagnosis cfDNA and bulk**
 1044 **breast tissue samples. (A-D)** Observed overlapping hypermethylated regions among predictor
 1045 cfDNA regions and significantly hypermethylated CpG sites (absolute difference > 0.1 & p <
 1046 0.0001) between **(A)** BRCA vs HBRNM, **(B)** ABRNM vs PBLs, **(C)** HBRNM vs PBLs **(D)** ABRNM
 1047 vs HBRNM in combined methylation array datasets (GSE133985, GSE74214, GSE88883,
 1048 GSE66313 & GSE101961). **(E-F)** Observed overlap between **(E)** BRCA vs ABRNM and **(F)** BRCA
 1049 vs HBRNM in 450k methylation array data from GSE69914. Bar plots represent observed number
 1050 of overlapping regions between cfDNA and bulk tissue, while significance of the overlap was
 1051 determined through a permutation test comparing the overlap between background regions in
 1052 cfDNA and significantly hypermethylated regions bulk tissue profiles (repeated 3000 times with

1053 random sets of subsampled cfDNA regions). Counts from background overlap are z-score
1054 normalized and shown in the boxplots. Points indicate the observed z-score normalized overlap
1055 with red indicating a significant overlap ($p < 0.01$) while gray points indicates non-significant
1056 overlaps ($p > 0.01$).
1057

Fig. S9



1058

1059 **Fig. S9: Genomic location of predictive pre-diagnosis cfDNA hypermethylated regions.**

1060 Proportion of hypermethylated regions across genomic annotations in **(A)** The predictor regions

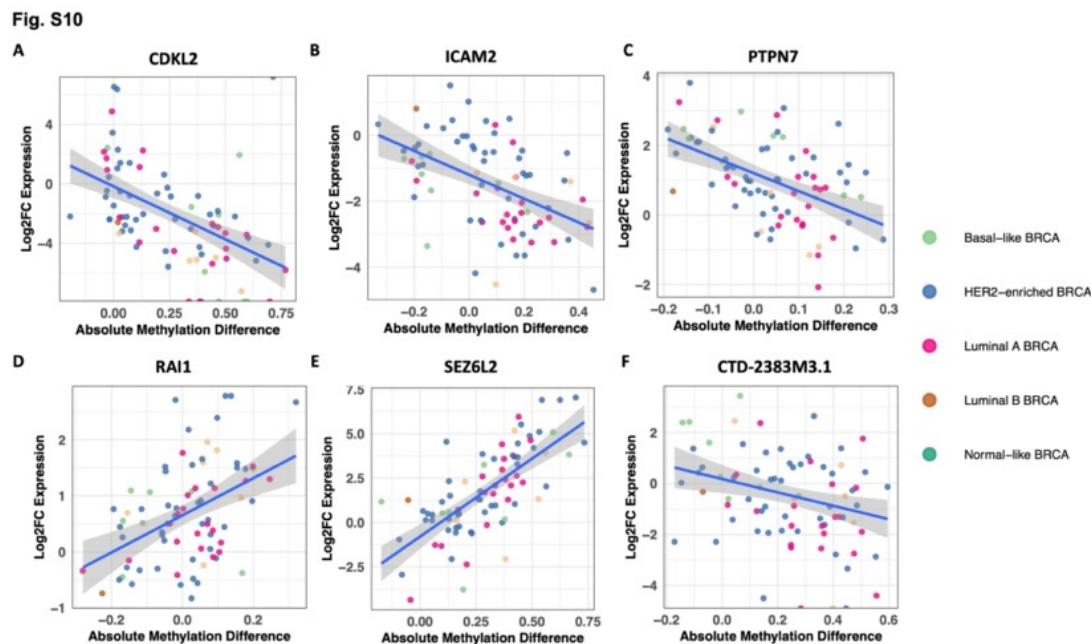
1061 comprised of the top 150 hypermethylated windows in discovery cohort, **(B)** predictor regions

1062 overlapping sites profiled by 450k DNA methylation array and **(C)** predictor regions overlapping

1063 sites profiled by 450k DNA methylation array that is also hypermethylated in bulk breast cancer

1064 tissue relative to PBLs or breast normal tissue.

1065



1066

1067 **Fig. S10: Hypermethylated regions in cfDNA associated with a change in gene expression.**

1068 Absolute change in promoter methylation and log₂ fold-change in gene expression between

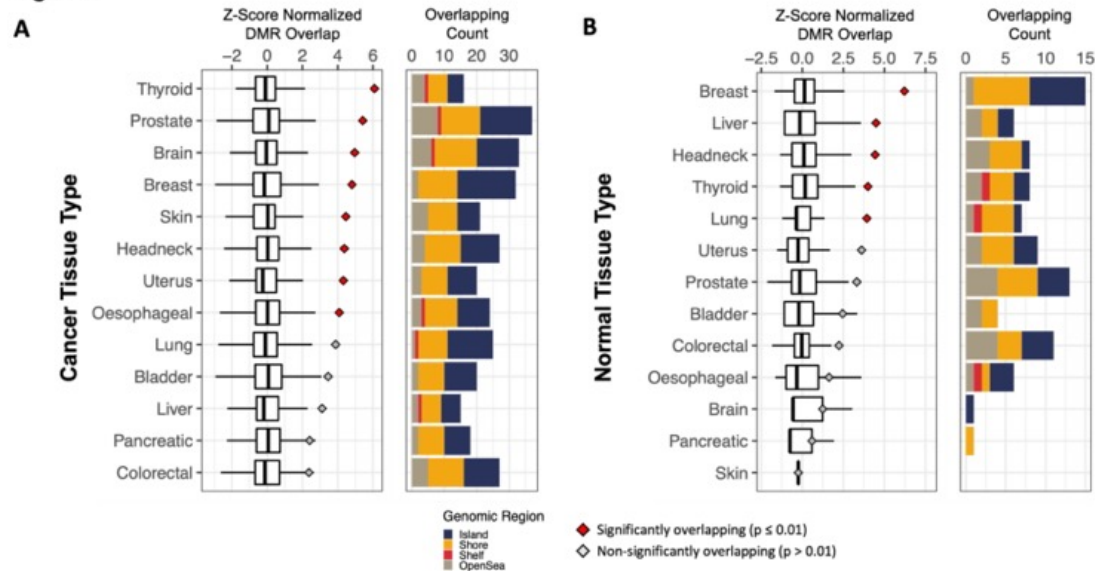
1069 TCGA breast cancer and adjacent breast normal tissue among the top 150 hypermethylated

1070 regions pre-diagnosis breast cancer cfDNA for **(A)** CDKL2, **(B)** ICAM2, **(C)** PTPN7, **(D)** RAI1, **(E)**

1071 SEZ6L2, **(F)** CTD-2383M3.1.

1072

Fig. S11



1073

1074 . S11: Overlapping hypermethylated regions between cfDNA and bulk cancer and normal

1075 tissue relative to PBLs. Differentially methylated CpG sites were identified between TCGA bulk

1076 adjacent normal versus PBLs for each tissue type using a standard F-test. Bar plots show the

1077 overlapping count of significantly hypermethylated regions (absolute difference > 0.1 and q-value

1078 < 0.001) in (A) bulk cancer tissue vs PBLs, and (B) bulk normal tissue vs PBLs that overlap with

1079 the top 150 cfDNA hypermethylated regions. Barplots are colored by genomic regions with blue

1080 representing CpG islands, yellow as shores, red as shelves and brown as open sea regions. The

1081 observed overlap was compared to the expected number of overlaps by computing the overlap

1082 between significant bulk tissue hypermethylated regions and randomly subsampled background

1083 cfDNA regions repeated 3000 times. The expected overlap are shown in box plots for 3000

1084 random subsampling iterations following z-score normalization, while the points illustrate the

1085 observed z-score normalized overlap with cfDNA hypermethylated regions. Red points indicate

1086 significant (p < 0.01) overlap between cfDNA hypermethylated regions and bulk tissue

1087 hypermethylated regions, while gray points indicate non-significant overlaps.

1088

1089

1090 **Supplementary Table 1: Baseline characteristics of pre-diagnosis cases and cancer-free**
1091 **control samples at time of blood collection.** Summary of age, sex, time since blood plasma
1092 collection, last mammogram prior to blood collection, ethnicity, body mass index (BMI), smoking
1093 frequency and alcohol consumption frequency among discovery and validation breast cancer
1094 cases and controls.

1095
1096 **Supplementary Table 2: Quality control, clinical and additional participant information**
1097 **across OHS samples.** Information across individual samples indicating age, CpG enrichment
1098 scores, methylated spike-in read proportions out of all methylation and non-methylation spike-in
1099 reads (thaliana beta), total reads following UMI deduplication, sample group, sample age, time
1100 between sample collection and diagnosis for cases, follow up time among controls, hormone
1101 receptor status of breast cancers and stage at diagnosis.

1102
1103 **Supplementary Table 3: Breast cancer cumulative incidence in OHS.** Cumulative incidence
1104 is presented as a function of time given a high (> 0.648) or low (< 0.648) classification score.
1105 Observed (Kaplan Meier) and predicted (Cox PH) probabilities are given stratified by risk score
1106 groups in discovery and validation samples.

1107
1108 **Supplementary Table 4: Genomic annotations across the top 150 hypermethylated**
1109 **predictor regions in pre-diagnosis cfDNA discovery set samples.** Genomic annotations
1110 performed using the Annotatr R package. Regions are also annotated to inform whether the
1111 region overlaps with sites on the 450k DNA methylation array and in hypermethylated bulk breast
1112 cancer tissue relative to PBLs and breast normal tissues.